Transportation Research Part B 167 (2023) 32–53

Contents lists available at ScienceDirect

Transportation Research Part B

journal homepage: www.elsevier.com/locate/trb

A mean-CVaR approach to the risk-averse single allocation hub location problem with flow-dependent economies of scale

Nader Ghaffarinasab [a,*], Özlem Çavuş [b], Bahar Y. Kara [b]

[a] Department of Industrial Engineering, University of Tabriz, Tabriz, Iran
[b] Department of Industrial Engineering, Bilkent University, Ankara, Turkey

ARTICLE INFO

Keywords:
Hub location
Risk-aversion
Economies of scale
Benders decomposition
Scenario grouping

ABSTRACT

The hub location problem (HLP) is a fundamental facility planning problem with various applications in transportation, logistics, and telecommunication systems. Due to strategic nature of the HLP, considering uncertainty and the associated risks is of high practical importance in designing hub networks. This paper addresses a risk-averse single allocation HLP, where the traffic volume between the origin–destination (OD) pairs is considered to be uncertain. The uncertainty in demands is captured by a finite set of scenarios, and a flow-dependent economies of scale scheme is used for transportation costs, modeled as a piece-wise concave function of flow on all network arcs. The problem is cast as a risk-averse two-stage stochastic problem using mean-CVaR as the risk measure, and a novel solution approach combining Benders decomposition and scenario grouping is proposed. An extensive set of computational experiments is conducted to study the effect of different input parameters on the optimal solution, and to evaluate the performance of the proposed solution algorithm. Managerial insights are derived and presented based on the obtained results.

1. Introduction

Hubs are intermediate facilities in transportation networks, where services such as transshipment, sorting, consolidation, etc. are provided. Rather than being directly connected, the origin–destination (OD) nodes interact with each other via one or more hubs in a hub network. The resulting network has fewer arcs through which more concentrated traffic flows are routed. Due to flow agglomeration on network arcs, transportation costs benefit from economies of scale. The aim of the hub location problem (HLP) is to locate the hub facilities and allocate the demand nodes to the hubs in order to route the OD traffic in a way that a certain criterion of interest (cost, service level, etc.) is optimized.

Hub networks can be classified into different types depending on how the non-hub nodes are assigned to the hubs. Two main allocation protocols are the single and multiple allocation schemes. In single allocation networks, the whole traffic sent and received by any non-hub node is routed via a single hub, whereas in multiple allocation networks, each non-hub node can receive and send flows via more than one hub. The single allocation scheme, which is used in the current work, constitutes the common topology in several real-life contexts such as the less-than-truckload (LTL) trucking industry, postal services, etc.

In the majority of the studies conducted on the HLP, it is assumed that the problem parameters and input values are known at the time of planning, and they are assumed to be fixed throughout the entire planning horizon. Nevertheless, perfect information is seldom available while making long-term decisions such as locating the hubs, and due to the volatile nature of business

* Corresponding author.
E-mail addresses: ngnasab@tabrizu.ac.ir (N. Ghaffarinasab), ozlem.cavus@bilkent.edu.tr (Ö. Çavuş), bkara@bilkent.edu.tr (B.Y. Kara).

https://doi.org/10.1016/j.trb.2022.11.008
Received 28 April 2022; Received in revised form 7 October 2022; Accepted 17 November 2022
Available online 29 November 2022

environments, information tends to change from time to time. Therefore, the decision maker faces a great deal of uncertainty regarding the problem data that stems from a number of factors such as population size shifts, cyclic fluctuations due to economic recession and expansion, technological developments, unexpected outbreak of diseases such as COVID-19, etc. In order to deal with uncertainty, stochastic programming has been used in the literature for the design of hub networks (see e.g., Contreras et al. (2011b), Alumur et al. (2012), Rostami et al. (2021)). However, in those studies the aim is to optimize the average performance of the system and the decision maker is assumed to be risk-neutral. Due to the fact that the HLP is a long-term non-repetitive problem, the risk-neutral approach may result in solutions which perform very poorly under some possible realizations of the uncertain parameters. Hence, adopting a risk-averse approach that focuses on the dispersion of random outcomes would yield solutions that are more robust toward data uncertainty.

In the classical modeling approaches to the HLP, economies of scale on transportation costs is modeled by a fixed flow-independent discount factor α ($0 \leq \alpha \leq 1$), which is only applied to inter-hub connections. In many realistic applications, however, it has been shown that the discount typically increases with volume of flow. For example, it has been found that costs per passenger-mile in air transportation decrease as the average load factor (number of passengers per flight) increases (McShan and Windle, 1989). On the other hand, detailed analysis of the optimal solutions of the classical models has revealed that the traffic on spoke arcs generally exceeds the traffic on hub arcs (Campbell, 2013). Therefore, simple flow-independent discount models not only miscalculate the transportation costs, but they also install hubs at sub-optimal locations. Economies of scale in hub-and-spoke networks are thus better approximated by a nonlinear cost function that allows costs to increase at a decreasing rate as flows increase (O'Kelly and Bryan, 1998). To overcome the computational difficulty of directly incorporating a nonlinear cost function, O'Kelly and Bryan (1998) proposed what they named as the FLOWLOC model, where they used a piecewise-linear concave function on the inter-hub links instead of the constant discount factor.

In an effort to address the above-mentioned drawbacks of the classical HLPs, this work introduces a risk-averse stochastic single allocation hub location problem with flow-dependent economies of scale, in which the traffic volume between the origin–destination (OD) pairs is assumed to be uncertain and the discount granted on transportation costs is a function of traffic volume. A finite set of scenarios is used to model the demand uncertainty, and the risk associated with the underlying random cost is measured using the mean-CVaR criterion. CVaR (Rockafellar and Uryasev, 2000) is a risk measure that is originally proposed for financial optimization, and has been extensively used in the literature. CVaR has also been used as a risk measure in different management and engineering contexts (Filippi et al., 2020). CVaR is a flexible risk measure in terms of risk-aversion, and by selecting a proper value for its parameters, it can be used to incorporate the risk preferences of different types of decision makers.

The contributions of this paper can be stated as follows:

- A risk-averse stochastic single allocation hub location problem with flow-dependent economies of scale is introduced;
- Piece-wise concave cost functions are used to capture economies of scale for the transportation costs on all network arcs;
- Mean-CVaR is used to measure the risks resulting from uncertain demands;
- The problem is cast as a two-stage stochastic program and formulated as an MILP model;
- An exact solution procedure based on Benders decomposition and scenario grouping is tailored for the problem;
- Extensive computational experiments have been conducted to study the effect of different input parameters and risk-aversion on the optimal solution and to demonstrate the efficiency of the proposed solution methods.

The remainder of this paper is organized as follows. The next section discusses the relevant literature for the problem at hand. In Section 3, mathematical formulations are developed for the problem. The proposed solution approach is detailed in Section 4. Computational experiments, and the obtained results are presented in Section 5. Finally, Section 6 concludes the paper and provides some outlooks for future research.

2. Literature review

The HLP was first introduced by O'Kelly (1986, 1987) and since then, numerous variants of it have been tackled by a large community of operations researchers. Interested reader is referred to Alumur and Kara (2008), Campbell and O'Kelly (2012), Farahani et al. (2013), Contreras and O'Kelly (2019), Alumur et al. (2021) for recent surveys on the HLP. This section presents a brief review on the related literature under three streams of research, as "hub location under uncertainty", "flow-dependent economies of scale in the HLP", and "Benders decomposition for the HLP".

2.1. Hub location under uncertainty

Addressing uncertainty in hub location has attracted more attention in recent years due to its high relevance to real-life contexts. Marianov and Serra (2003) propose a queuing model for a hub location in air transport setting. Yang (2009) develops a two-stage stochastic program for an HLP with uncertain demands, also in the context of airline transportation. Sim et al. (2009) tackle the HLP with stochastic travel times to limit the probability of travel time exceeding a given threshold by using chance constraints. Contreras et al. (2011b) study the stochastic uncapacitated hub location problems with uncertain demands and transportation costs. Zhai et al. (2012) address a class of two-stage stochastic HLPs with uncertain demands by using a minimum-risk criterion. Alumur et al. (2012) consider set-up cost and demand as two sources of uncertainty in the stochastic HLPs. Chaharsooghi et al. (2017) tackle an uncertain HLP with unreliable hubs as a two-stage stochastic program. Correia et al. (2018) study a multi-period stochastic capacitated multiple allocation hub location problems with demand uncertainty. Azizi et al.

(2018) propose a model for the design of hub-and-spoke networks under stochastic demand and congestion. Peiró et al. (2019) address an uncapacitated r-allocation p-hub median problem with direct shipment option under demand and transportations cost uncertainty. Taherkhani et al. (2020) address the profit-maximizing hub location with stochastic demands by considering multiple demand classes. In a follow-up work, Taherkhani et al. (2021) extend their work to include uncertain revenues. Rostami et al. (2021) study a single allocation hub location under demand uncertainty using two types of modeling strategies, namely the fixed and variable allocation strategies. Shang et al. (2021) introduce a stochastic multi-modal hub location problem with direct link strategy and multiple capacity levels for cargo delivery systems under demand uncertainty.

Robust optimization is another technique used to address uncertainty in HLPs. Shahabi and Unnikrishnan (2014) consider a robust HLP under demand uncertainty. Capacitated robust single and multiple allocation HLPs under demand uncertainty are studied in Ghaffari-Nasab et al. (2015). Meraklı and Yaman (2016) study a robust multiple allocation HLP under polyhedral demand uncertainty. Zetina et al. (2017) present robust counterparts for a multiple allocation HLP where the level of conservatism is adjusted by a budget of uncertainty. de Sá et al. (2018a,b) study robust multiple allocation incomplete hub location problem with and without service time requirements. Ghaffarinasab (2018) proposes an efficient metaheuristic for solving three variants of the robust multiple allocation p-hub median problem under polyhedral demand uncertainty. In another paper, Ghaffarinasab et al. (2019) tackle the single allocation p-hub median problem under hose and hybrid demand uncertainty. A capacitated multiple allocation hub location problem under hose demand uncertainty is addressed by Meraklı and Yaman (2017).

Risk management techniques have been used to deal with a spectrum of uncertain optimization problems. Conditional value-at-risk (CVaR) is arguably the most popular risk measure. Despite the fact that CVaR was originally employed for risk minimization in financial markets, during the last decade it has been applied to different problems beyond finance (Filippi et al., 2020). Yu et al. (2017) address a resilient facility location problem where the facilities are subject to random disruptions using CVaR as the risk measure. Elçi and Noyan (2018) study a stochastic pre-disaster relief network design problem with CVaR. Noyan (2012) proposes a risk-averse two-stage stochastic program for a disaster management application, with CVaR as the risk measure. Hosseini and Verma (2018) use CVaR to model the risk involved in routing rail hazmat shipments. A multi-objective multi-echelon supply chain network design problem is addressed by Golpîra et al. (2017), where the risk resulting from demand uncertainty is taken into account by CVaR measure. In the context of hub location, Kargar and Mahmutoğulları (2022) propose risk-averse two-stage stochastic formulations for the uncapacitated multiple allocation p-hub median problem using CVaR and mean-CVaR risk measures. Using a closely-related measure of risk, called conditional β-mean, three basic variants of multiple allocation HLP are addressed by Ghaffarinasab and Kara (2022). There are also few works in the literature that have applied the concept of value-at-risk (VaR), another strongly related risk measure to CVaR, to model different variants of the HLP (Yang et al., 2014, 2017; Ghezavati and Hosseinifar, 2018).

2.2. Flow-dependent economies of scale

In most of the HLPs, the discount on transportation costs is modeled using a fixed flow-independent factor α, where $0 \leq \alpha \leq 1$. However, some authors have relaxed this naive assumption and assumed that the discount granted on the transportation costs is a function of the flow to be routed on each arc. O'Kelly and Bryan (1998) consider a flow-dependent model for economies of scale represented by a piece-wise concave linear function of the traffic. Klincewicz (2012) devise a specialized optimal enumeration procedure, some greedy random adaptive search procedures (GRASP), and tabu search based heuristics and use test instances with at most 25 nodes. Racunica and Wynter (2005) consider a piece-wise linear concave cost function on inter-hub connections and on spokes. However, the linearization of the proposed model includes a large number of binary variables even for small-size instances.

Kimms (2006) proposes three multiple allocation p-hub median problems with direct service and with fixed and variable costs. The aim is to optimize the number of vehicles used on each arc of a fully interconnected hub network. de Camargo et al. (2009b) develop a model containing variables associated with each cost segment and path combination. O'Kelly et al. (2015) formulate a model to analyze the role of fixed costs in the design of optimal transportation hub networks. Their work allows particular versions of hub networks to emerge from the cost structure, rather than imposing a rigid predefined connectivity protocol. Similarly, Campbell et al. (2015) focus on a hub location and network design problem with fixed and variable transportation costs on all arcs. They consider fixed costs for the hubs and allow direct shipments. Tanash et al. (2017) study a modular hub location problem with flow dependent transportation costs, which are based on modular arc costs. More recently, Lüer-Villagra et al. (2019) study the single allocation p-hub median problem with piece-wise linear costs on all network arcs. The authors develop a math-heuristic solution procedure for solving large instances of the problem. Alkaabneh et al. (2019) present a single allocation HLP with flow-dependent economies of scale on inter-hub connections and congestion at hubs. In a related work, Najy and Diabat (2020) address the multiple allocation version of the problem. Rostami et al. (2022) address the single allocation hub location problem with heterogeneous economies of scale where the discount on transportation cost is a function of the traffic on the network arcs.

2.3. Benders decomposition for the HLP

Benders decomposition (BD) (Benders, 1962) is a partitioning method which has been successfully applied to different variants of the HLP in the literature. de Camargo et al. (2008) use BD algorithms to solve the uncapacitated multiple allocation hub location problem (UMAHLP). Gelareh and Nickel (2008) propose a BD procedure for HLPs arising in public transport. Another BD algorithm is devised by de Camargo et al. (2009b) for the HLPs with flow-dependent discount factor. Generalized BD algorithms are developed for HLPs under congestion by de Camargo et al. (2009a, 2011). Contreras et al. (2011a) use BD algorithms to solve large-scale instances of the UMAHLP. The same authors propose a BD algorithm for solving stochastic uncapacitated HLPs (Contreras et al., 2011b). An

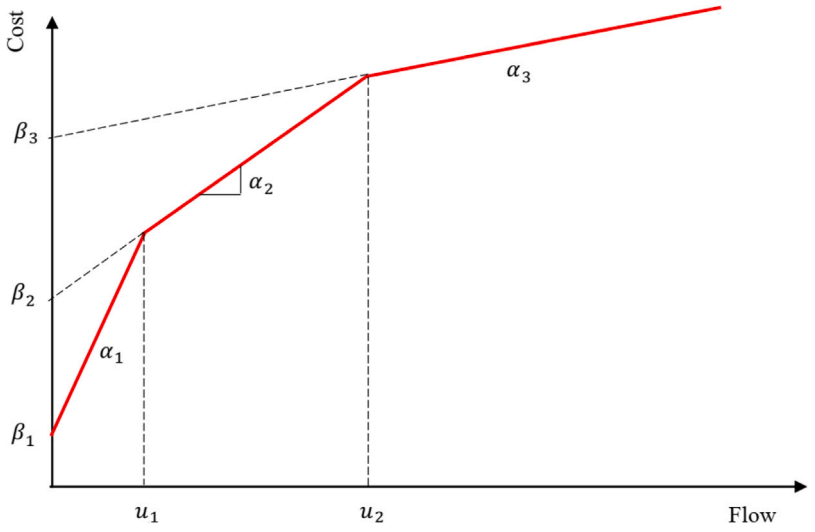

Fig. 1. Transportation cost on network arcs as a piece-wise linear concave function of flow volume.

accelerated BD procedure is presented by Gelareh and Nickel (2011) for an HLP in the context of urban transport and liner shipping network design. This work is then extended to solve a multi-period HLP under budget constraints (Gelareh et al., 2015). Contreras et al. (2012) use BD algorithm to solve capacitated version of the HLPs. de Camargo et al. (2013) apply a BD algorithm for the many-to-many hub location routing problem. The tree of hubs location problem and the hub line location problem are solved by BD algorithm by de Sá et al. (2013, 2015), respectively. O'Kelly et al. (2015) present a BD algorithm to solve the HLP with price-sensitive demands. Meraklı and Yaman (2016) propose two BD procedures for the robust uncapacitated multiple allocation p-hub median problem (UMApHMP) under polyhedral demand uncertainty. BD algorithms are developed by Ghaffarinasab (2022) for a similar robust HLP with adjustable conservatism level. de Sá et al. (2018a,b) propose BD algorithms for solving the robust incomplete hub location problem with uncertain parameters. Ghaffarinasab and Kara (2019) develop BD algorithms for solving uncapacitated single allocation HLPs with fixed and variable number of hubs. Taherkhani et al. (2020) design a BD procedure to solve hub location problems with profit maximization. Efficient BD algorithm for solving variants of the uncapacitated multiple allocation p-hub center problem (UMApHCP) are proposed by Ghaffarinasab (2020) and Ghaffarinasab et al. (2022). Najy and Diabat (2020) develop a BD algorithm for a multiple allocation HLP with flow-dependent economies of scale on inter-hub connections and congestion at hub facilities. Benders-based heuristic algorithms are designed for solving a multiple allocation tree of hubs location problem for non-complete networks in Kayışoğlu and Akgün (2021).

Observing the literature, we conclude that so far the HLP has not been addressed by incorporating uncertainty and simultaneously assuming flow-dependent economies of scale using mean-CVaR risk measure. Furthermore, carefully designed BD algorithms have been proved to be an effective solution approach for many HLPs. Therefore, in this work, we propose mean-CVaR approach to the risk-averse single allocation hub location problem with flow-dependent economies of scale and develop an efficient solution algorithm based on Benders decomposition and scenario grouping.

3. Mathematical formulation

Let $G = (N, A)$ be a network with N and A denoting its sets of nodes and arcs, respectively. The fixed cost of opening a hub at node $k \in N$ is represented by f_k. For all $i, j \in N$, let w_{ij} denote the amount of flow originated at node i and destined to node j, and d_{ij} denote the distance between nodes i and j. We model the transportation cost on all arcs of the network as a piece-wise linear concave function of flow volume as shown in Fig. 1.

Assume that Q is the set of discount intervals, and l_q and u_q respectively represents the lower and upper limits of the discount interval $q \in Q$ in our cost function (note that $u_q = l_{q+1}$ for all $q \in Q$). Moreover, let β_q and α_q, respectively, denote the intercept and slope of the corresponding line segments in the interval $q \in Q$ of the cost function. For each node $i \in N$, let c_i^o denote the unit transportation cost for the outgoing traffic from node i over the spoke arc connecting it to its assigned hub, and c_i^d denote the unit transportation cost for the incoming traffic to node i via the same spoke arc but in the reverse direction. Due to single assignment assumption, the transportation costs corresponding to the spoke links connecting each non-hub node $i \in N$ to any hub node $k \in N$ can be determined *a priori* and we denote this cost as $c_{ik} = (c_i^o + c_i^d)d_{ik}$. Let the binary variable h_k be 1 if node $i \in N$ is selected as hub; and 0, otherwise. Moreover, the binary variable x_{ik} is used to take the value of 1 if node $i \in N$ is assigned to hub $k \in N$; and 0, otherwise. The non-negative variable y_{ijkmq} denotes the fraction of flow originated at node $i \in N$ and destined to node $j \in N$ that is routed through the arc connecting the hubs $k \in N$ and $m \in N$ using the cost interval $q \in Q$. Finally, let the binary variable z_{kmq} be 1 if the flow on the inter-hub arc (k, m) satisfies the discount level $q \in Q$; and 0, otherwise. The problem consists of the

selection of a set of hub nodes and determining how the non-hub nodes will be assigned to the hubs and the OD flows will be routed through the network so that total facility location and transportation cost is minimized. The MIP model for the deterministic single allocation hub location problem with flow-dependent economies of scale (SAHLP-FD) can be written as:

$$\min \sum_{k\in N} f_k h_k + \sum_{i\in N}\sum_{k\in N} c_{ik}x_{ik} + \sum_{k\in N}\sum_{m\in N}\sum_{q\in Q} d_{km}\beta_q z_{kmq} + \sum_{i\in N}\sum_{j\in N}\sum_{k\in N}\sum_{m\in N}\sum_{q\in Q} w_{ij}d_{km}\alpha_q y_{ijkmq} \tag{1}$$

$$\text{s.t.:} \sum_{k\in N} x_{ik} = 1 \qquad \forall i \in N \tag{2}$$

$$x_{ik} \le h_k \qquad \forall i,k \in N \tag{3}$$

$$\sum_{m\in N}\sum_{q\in Q} y_{ijkmq} = x_{ik} \qquad \forall i,j,k \in N \tag{4}$$

$$\sum_{k\in N}\sum_{q\in Q} y_{ijkmq} = x_{jm} \qquad \forall i,j,m \in N \tag{5}$$

$$\sum_{q\in Q} z_{kmq} \ge h_k + h_m - 1 \qquad \forall k,m \in N \tag{6}$$

$$\sum_{i\in N}\sum_{j\in N} w_{ij} y_{ijkmq} \le u_q z_{kmq} \qquad \forall k,m \in N, q \in Q \tag{7}$$

$$h_k \in \{0,1\} \qquad \forall k \in N \tag{8}$$

$$x_{ik} \in \{0,1\} \qquad \forall i,k \in N \tag{9}$$

$$z_{kmq} \in \{0,1\} \qquad \forall k,m \in N, q \in Q \tag{10}$$

$$y_{ijkmq} \ge 0 \qquad \forall i,j,k,m \in N, q \in Q \tag{11}$$

The objective function (1) minimizes the total facility location and transportation costs. Constraints (2) ensure that every node is assigned to exactly one hub. Constraints (3) imply that no node is assigned to a site unless a hub is opened at that site. Constraints (4) state that if node $i \in N$ is assigned to hub $k \in N$, all the outgoing flow corresponding to node i aiming to a specific node $j \in N$ must go through some hub $m \in N$. Similarly, constraints (5) imply that the incoming flow to a node $j \in N$ assigned to hub $m \in N$ from any node $i \in N$ must be transferred using some hub $k \in N$. Constraints (6) state that if both nodes $k, m \in N$ are selected as hub nodes, one segment $q \in Q$ for arc (k,m) has to be activated. The appropriate discount factor to each inter-hub arc based on the corresponding flow volumes is set by (7). Finally, (8)–(11) are the standard domain constraints for the decision variables.

Let $(\Omega, \mathcal{F}, P)$ be some probability space, $X : \Omega \to \mathbb{R}$ be an $\mathcal{F}$-measurable function (a random variable) for which lower values are preferable, and $\mathcal{X}$ be a space of functions $X(\cdot)$. A real-valued function $\rho : \mathcal{X} \to \mathbb{R}$ satisfying the following axioms is called a coherent measure of risk.

(A1) Convexity: $\rho(\lambda X + (1-\lambda)Y) \le \lambda\rho(X) + (1-\lambda)\rho(Y)$ for all $X, Y \in \mathcal{X}$ and $\lambda \in [0,1]$,
(A2) Monotonicity: $X \succeq Y$ implies $\rho(X) \ge \rho(Y)$ for all $X, Y \in \mathcal{X}$,
(A3) Translational Equivariance: $\rho(X + a) = \rho(X) + a$ for all $a \in \mathbb{R}$ and $X \in \mathcal{X}$,
(A4) Positive Homogeneity: $\rho(aX) = a\rho(X)$ for all $a > 0$ and $X \in \mathcal{X}$.

Here, $X \succeq Y$ implies that $X(\omega) \ge Y(\omega)$ for a.e. $\omega \in \Omega$. The coherent risk measures along with their axiomatic properties are introduced in the seminal paper of Artzner et al. (1999) and further extended by Delbaen (2002).

Conditional Value-at-Risk (CVaR), which has been used extensively in the literature, is an important coherent measure of risk. For a random variable $X \in \mathcal{X}$, the conditional value-at-risk at confidence level $\gamma \in [0,1)$ is related to the expectation of X under the condition that it exceeds the γ-quantile threshold, and is defined as (see Rockafellar and Uryasev (2002)):

$$CVaR_\gamma(X) := \min\left\{\eta + \frac{1}{1-\gamma}\mathbb{E}[(X-\eta)_+] : \eta \in \mathbb{R}\right\} \tag{12}$$

where $(a)_+ := \max\{a, 0\}$. In fact, the minimum in (12) is attained at the γ-quantile, which is known as the value-at-risk (VaR) at confidence level γ as $VaR_\gamma(X) := \min\{\eta \in \mathbb{R} : P(X \le \eta) \ge \gamma\}$.

In this study, we focus on another coherent risk measure $\rho : \mathcal{X} \to \mathbb{R}$, which is a weighted average of CVaR and expected value:

$$\rho(X) := \lambda CVaR_\gamma(X) + (1-\lambda)\mathbb{E}[X], \quad \lambda \in [0,1]. \tag{13}$$

Now we extend the model (1)–(11) to include uncertainty in the demand flows from a risk-averse decision maker's perspective. Let Ω be the set of all possible scenarios representing demand realizations, and assume that p^ω denotes the occurrence probability of scenario $\omega \in \Omega$. Under each scenario ω, the realized demand flow between nodes $i, j \in N$ is denoted by w_{ij}^ω, and the transportation cost on spoke arc (i,k), $i,k \in N$ is represented by c_{ik}^ω. In a two-stage stochastic programming setting, the decisions regarding the location of hubs are taken in the first stage, while the decisions regarding the assignment of nodes and routing of flows are made in the second stage. Therefore, the decision variables x_{ik}^ω, y_{ijkmq}^ω, and z_{kmq}^ω represent the previously defined variables taken under the

scenario $\omega \in \Omega$. Since the location decisions are determined before observing the uncertainty, the associated decision variables h_k, $k \in N$ are not indexed with scenario.

The mean-CVaR formulation for the risk-averse single allocation HLP with flow-dependent economies of scale (RASAHLP-FD) can now be written as:

$$\min \sum_{k\in N} f_k h_k + \lambda\left(\eta + \frac{1}{1-\gamma}\sum_{\omega\in\Omega} p^\omega v^\omega\right) + (1-\lambda)\sum_{\omega\in\Omega} p^\omega\left(\sum_{i\in N}\sum_{k\in N} c^\omega_{ik}x^\omega_{ik} + \sum_{k\in N}\sum_{m\in N}\sum_{q\in Q} d_{km}\beta_q z^\omega_{kmq} + \sum_{i\in N}\sum_{j\in N}\sum_{k\in N}\sum_{m\in N}\sum_{q\in Q} w^\omega_{ij} d_{km}\alpha_q y^\omega_{ijkmq}\right) \tag{14}$$

s.t.:
$$v^\omega \geq \sum_{i\in N}\sum_{k\in N} c^\omega_{ik}x^\omega_{ik} + \sum_{k\in N}\sum_{m\in N}\sum_{q\in Q} d_{km}\beta_q z^\omega_{kmq} + \sum_{i\in N}\sum_{j\in N}\sum_{k\in N}\sum_{m\in N}\sum_{q\in Q} w^\omega_{ij} d_{km}\alpha_q y^\omega_{ijkmq} - \eta \qquad \forall \omega \in \Omega \tag{15}$$

$$\sum_{k\in N} x^\omega_{ik} = 1 \qquad \forall i \in N, \omega \in \Omega \tag{16}$$

$$x^\omega_{ik} \leq h_k \qquad \forall i,k \in N, \omega \in \Omega \tag{17}$$

$$\sum_{m\in N}\sum_{q\in Q} y^\omega_{ijkmq} = x^\omega_{ik} \qquad \forall i,j,k \in N, \omega \in \Omega \tag{18}$$

$$\sum_{k\in N}\sum_{q\in Q} y^\omega_{ijkmq} = x^\omega_{jm} \qquad \forall i,j,m \in N, \omega \in \Omega \tag{19}$$

$$\sum_{q\in Q} z^\omega_{kmq} \geq h_k + h_m - 1 \qquad \forall k,m \in N, \omega \in \Omega \tag{20}$$

$$\sum_{i\in N}\sum_{j\in N} w^\omega_{ij} y^\omega_{ijkmq} \leq u_q z^\omega_{kmq} \qquad \forall k,m \in N, q \in Q, \omega \in \Omega \tag{21}$$

$$h_k \in \{0,1\} \qquad \forall k \in N \tag{22}$$

$$x^\omega_{ik} \in \{0,1\} \qquad \forall i,k \in N, \omega \in \Omega \tag{23}$$

$$z^\omega_{kmq} \in \{0,1\} \qquad \forall k,m \in N, q \in Q, \omega \in \Omega \tag{24}$$

$$y^\omega_{ijkmq} \geq 0 \qquad \forall i,j,k,m \in N, q \in Q, \omega \in \Omega \tag{25}$$

$$v^\omega \geq 0 \qquad \forall \omega \in \Omega \tag{26}$$

$$\eta \in \mathbb{R} \tag{27}$$

The second and third terms in the objective function (14), respectively, represent the CVaR and expected value of the second-stage transportation costs. The total facility location cost is moved out of mean-CVaR risk measure due to axiom (A3). Note that, in the model, the CVaR risk measure (12) is linearized using constraints (15) and (26)–(27) and auxiliary variables η and v^ω. In particular, the optimal value of η gives the value-at-risk at confidence level γ, and optimal v^ω represents the positive part of the total transportation cost under scenario ω minus the value of η (as calculated in the right-hand-side of (15)). In the above formulation, the parameters $\lambda \in [0,1]$ and $\gamma \in [0,1)$ reflect the preference of the decision maker toward risk. In other words, when $\lambda = 0$ we have the risk-neutral problem where the network configuration is designed solely based on the expected cost of the system, whereas $\lambda = 1$ results in a pure CVaR model compatible with a risk-averse decision maker's perspective. The intermediate values of λ enable us to make a trade-off between the mean and CVaR values. Also, when γ increases, the decision maker is expected to become more risk-averse.

4. Solution procedure

Benders decomposition (BD) (Benders, 1962) is an exact solution procedure for large-scale MIP models in which the problem is decomposed in such a way that the complicating variables form a master problem (MP) and the remaining variables constitute the subproblem (SP). The problem is then solved using a cutting plane approach where the cuts extracted from solving the SP are iteratively added to the MP. In this work we develop a hybrid solution procedure combining BD and scenario grouping (SG) technique (Ahmed, 2013; Sandıkçı et al., 2013) for solving the RASAHLP-FD. In classical implementation of BD algorithm, we need to solve the master problem at each iteration. However, we use a modern implementation within a branch-and-cut (B&C) setting where the MP is solved in one attempt and the cuts are added on the fly by using the capabilities of the state-of-the-art solvers. We separate the Benders cuts every time we visit a candidate integer solution in the B&C tree of the MP. Therefore, the computational effort needed to solve an integer problem at each iteration is considerably reduced. Since the solution times increase by including larger number of scenarios, we also employ SG as a divide-and-conquer scheme to decompose the set of scenarios into smaller groups that can be solved more efficiently in terms of the computational time and resources. The remainder of this section presents more details on the proposed hybrid algorithm for solving the RASAHLP-FD.

4.1. Benders reformulation

By fixing the vectors of binary location and allocation variables as $(\boldsymbol{h}, \boldsymbol{x}) = (\hat{\boldsymbol{h}}, \hat{\boldsymbol{x}})$ in model (14)–(27), the subproblem corresponding to scenario $\omega \in \Omega$ can be written as:

$(\mathbf{SP}^{\omega})$

$$\phi^{\omega}(\hat{\boldsymbol{h}}, \hat{\boldsymbol{x}}) = \min \sum_{k\in N}\sum_{m\in N}\sum_{q\in Q} d_{km}\beta_q z^{\omega}_{kmq} + \sum_{i\in N}\sum_{j\in N}\sum_{k\in N}\sum_{m\in N}\sum_{q\in Q} w^{\omega}_{ij} d_{km}\alpha_q y^{\omega}_{ijkmq} \tag{28}$$

$$\text{s.t.:} \sum_{m\in N}\sum_{q\in Q} y^{\omega}_{ijkmq} = \hat{x}^{\omega}_{ik} \qquad \forall i,j,k \in N \tag{29}$$

$$\sum_{k\in N}\sum_{q\in Q} y^{\omega}_{ijkmq} = \hat{x}^{\omega}_{jm} \qquad \forall i,j,m \in N \tag{30}$$

$$\sum_{q\in Q} z^{\omega}_{kmq} \geq \hat{h}_k + \hat{h}_m - 1 \qquad \forall k,m \in N \tag{31}$$

$$\sum_{i\in N}\sum_{j\in N} w^{\omega}_{ij} y^{\omega}_{ijkmq} \leq u_q z^{\omega}_{kmq} \qquad \forall k,m \in N, q \in Q \tag{32}$$

$$z^{\omega}_{kmq} \in \{0,1\} \qquad \forall k,m \in N, q \in Q \tag{33}$$

$$y^{\omega}_{ijkmq} \geq 0 \qquad \forall i,j,k,m \in N, q \in Q \tag{34}$$

By introducing the variable θ^{ω} as a surrogate for the inter-hub transportation cost under scenario $\omega \in \Omega$, the resulting master problem reads as:

$$\min \sum_{k\in N} f_k h_k + \lambda\left(\eta + \frac{1}{1-\gamma}\sum_{\omega\in\Omega} p^{\omega} v^{\omega}\right) + (1-\lambda)\sum_{\omega\in\Omega} p^{\omega}\left(\sum_{i\in N}\sum_{k\in N} c^{\omega}_{ik} x^{\omega}_{ik} + \theta^{\omega}\right) \tag{35}$$

s.t.: (16), (17), (22), (23), (26), (27)

$$\theta^{\omega} \geq \phi^{\omega}(\boldsymbol{h}, \boldsymbol{x}) \qquad \forall \omega \in \Omega \tag{36}$$

$$v^{\omega} \geq \sum_{i\in N}\sum_{k\in N} c^{\omega}_{ik} x^{\omega}_{ik} + \theta^{\omega} - \eta \qquad \forall \omega \in \Omega \tag{37}$$

$$\theta^{\omega} \geq 0 \qquad \forall \omega \in \Omega \tag{38}$$

where $\phi^{\omega}(\boldsymbol{h}, \boldsymbol{x})$ represents the inter-hub transportation cost for a given pair of location and allocation vectors $(\boldsymbol{h}, \boldsymbol{x})$ under scenario $\omega \in \Omega$, provided by solving the MILP subproblem (28)–(34).

Note that since the allocation decisions (represented by $\boldsymbol{x}$ variables) are determined by the MP, for each inter-hub connection (k,m) under scenario ω, we can readily calculate the corresponding flow volume F^{ω}_{km} as follows:

$$F^{\omega}_{km} = \sum_{i\in N}\sum_{j\in N} w^{\omega}_{ij} \hat{x}^{\omega}_{ik} \hat{x}^{\omega}_{jm} \tag{39}$$

Given the flow volume on each inter-hub connection (k,m) we can determine the corresponding flow segment under scenario ω as $\hat{q}^{\omega}_{km}$. Therefore, the subproblem can be rewritten as:

$(\mathbf{SP}^{\omega\hat{q}})$

$$\phi^{\omega}(\hat{\boldsymbol{h}}, \hat{\boldsymbol{x}}) = \min \sum_{k\in N}\sum_{m\in N} d_{km}\beta_{\hat{q}^{\omega}_{km}} z^{\omega}_{km\hat{q}^{\omega}_{km}} + \sum_{i\in N}\sum_{j\in N}\sum_{k\in N}\sum_{m\in N} w^{\omega}_{ij} d_{km}\alpha_{\hat{q}^{\omega}_{km}} y^{\omega}_{ijkm\hat{q}^{\omega}_{km}} \tag{40}$$

$$\text{s.t.:} \sum_{m\in N} y^{\omega}_{ijkm\hat{q}^{\omega}_{km}} = \hat{x}^{\omega}_{ik} \qquad \forall i,j,k \in N \tag{41}$$

$$\sum_{k\in N} y^{\omega}_{ijkm\hat{q}^{\omega}_{km}} = \hat{x}^{\omega}_{jm} \qquad \forall i,j,m \in N \tag{42}$$

$$z^{\omega}_{km\hat{q}^{\omega}_{km}} \geq \hat{h}_k + \hat{h}_m - 1 \qquad \forall k,m \in N \tag{43}$$

$$z^{\omega}_{km\hat{q}^{\omega}_{km}} \in \{0,1\} \qquad \forall k,m \in N \tag{44}$$

$$y^{\omega}_{ijkm\hat{q}^{\omega}_{km}} \geq 0 \qquad \forall i,j,k,m \in N \tag{45}$$

Note that constraints (32) are not included in $SP^{\omega\hat{q}}$ as their role was to determine the appropriate discount factor to each inter-hub connection which is now available by the indices $\hat{q}^{\omega}_{km}$. The subproblem $SP^{\omega\hat{q}}$ can now be decomposed into two smaller problems with respect to $\boldsymbol{y}$ and $\boldsymbol{z}$ variables as $SP^{\omega\hat{q}}_{y}$ and $SP^{\omega\hat{q}}_{z}$, respectively:

($\mathbf{SP}^{\omega\hat{q}}_{y}$)

$$\phi^{\omega}_{y}(\hat{\boldsymbol{h}},\hat{\boldsymbol{x}}) = \min \sum_{i\in N}\sum_{j\in N}\sum_{k\in N}\sum_{m\in N} w^{\omega}_{ij} d_{km} \alpha_{\hat{q}^{\omega}_{km}} y^{\omega}_{ijkm\hat{q}^{\omega}_{km}} \tag{46}$$

$$\text{s.t.:} \sum_{m\in N} y^{\omega}_{ijkm\hat{q}^{\omega}_{km}} = \hat{x}^{\omega}_{ik} \qquad \forall i,j,k \in N \tag{47}$$

$$\sum_{k\in N} y^{\omega}_{ijkm\hat{q}^{\omega}_{km}} = \hat{x}^{\omega}_{jm} \qquad \forall i,j,m \in N \tag{48}$$

$$y^{\omega}_{ijkm\hat{q}^{\omega}_{km}} \geq 0 \qquad \forall i,j,k,m \in N \tag{49}$$

($\mathbf{SP}^{\omega\hat{q}}_{z}$)

$$\phi^{\omega}_{z}(\hat{\boldsymbol{h}},\hat{\boldsymbol{x}}) = \min \sum_{k\in N}\sum_{m\in N} d_{km}\beta_{\hat{q}^{\omega}_{km}} z^{\omega}_{km\hat{q}^{\omega}_{km}} \tag{50}$$

$$\text{s.t.:} \; z^{\omega}_{km\hat{q}^{\omega}_{km}} \geq \hat{h}_k + \hat{h}_m - 1 \qquad \forall k,m \in N \tag{51}$$

$$z^{\omega}_{km\hat{q}^{\omega}_{km}} \in \{0,1\} \qquad \forall k,m \in N \tag{52}$$

where $\phi^{\omega}_{y}(\hat{\boldsymbol{h}},\hat{\boldsymbol{x}}) + \phi^{\omega}_{z}(\hat{\boldsymbol{h}},\hat{\boldsymbol{x}}) = \phi^{\omega}(\hat{\boldsymbol{h}},\hat{\boldsymbol{x}})$. The special structure of $SP^{\omega\hat{q}}_{z}$ allows us to relax the integrality of the $\boldsymbol{z}$ variables leaving us with the following linear programming problem:

($\mathbf{SP}^{\omega\hat{q}}_{zRX}$)

$$\phi^{\omega}_{z}(\hat{\boldsymbol{h}},\hat{\boldsymbol{x}}) = \min \sum_{k\in N}\sum_{m\in N} d_{km}\beta_{\hat{q}^{\omega}_{km}} z^{\omega}_{km\hat{q}^{\omega}_{km}} \tag{53}$$

$$\text{s.t.:} \; z^{\omega}_{km\hat{q}^{\omega}_{km}} \geq \hat{h}_k + \hat{h}_m - 1 \qquad \forall k,m \in N \tag{54}$$

$$z^{\omega}_{km\hat{q}^{\omega}_{km}} \geq 0 \qquad \forall k,m \in N \tag{55}$$

Because of the minimization sense in the objective function (53), for each pair (k,m), whenever both k and m are hubs, the variable $z^{\omega}_{km\hat{q}^{\omega}_{km}}$ will take the value of 1; otherwise, it will be 0. Therefore, we now have two linear programming problems as subproblems for our main problem.

Let σ^{ω}_{ijk} and μ^{ω}_{ijm} be the dual variables associated with constraints (47) and (48) in $SP^{\omega\hat{q}}_{y}$, respectively. The corresponding dual subproblem (DSP^{ω}_{y}) can now be written as:

($\mathbf{DSP}^{\omega}_{y}$)

$$\max \sum_{i\in N}\sum_{j\in N}\sum_{k\in N} \hat{x}^{\omega}_{ik}\sigma^{\omega}_{ijk} + \sum_{i\in N}\sum_{j\in N}\sum_{m\in N} \hat{x}^{\omega}_{jm}\mu^{\omega}_{ijm} \tag{56}$$

$$\text{s.t.:} \; \sigma^{\omega}_{ijk} + \mu^{\omega}_{ijm} \leq w^{\omega}_{ij} d_{km} \alpha_{\hat{q}^{\omega}_{km}} \qquad \forall i,j,k,m \in N \tag{57}$$

$$\sigma^{\omega}_{ijk}, \mu^{\omega}_{ijm} \in \mathbb{R} \qquad \forall i,j,k,m \in N \tag{58}$$

Furthermore, let δ^{ω}_{km} be the dual variables associated with constraints (54) in $SP^{\omega\hat{q}}_{zRX}$. The dual subproblem (DSP^{ω}_{z}) can be stated as:

($\mathbf{DSP}^{\omega}_{z}$)

$$\max \sum_{k\in N}\sum_{m\in N} (\hat{h}_k + \hat{h}_m - 1)\delta^{\omega}_{km} \tag{59}$$

$$\text{s.t.:} \; \delta^{\omega}_{km} \leq d_{km}\beta_{\hat{q}^{\omega}_{km}} \qquad \forall k,m \in N \tag{60}$$

$$\delta^{\omega}_{km} \geq 0 \qquad \forall k,m \in N \tag{61}$$

Finally, the master problem for the RASAHLP-FD solves the following MIP model:

(**MP**)

$$\min \sum_{k\in N} f_k h_k + \lambda\left(\eta + \frac{1}{1-\gamma}\sum_{\omega\in\Omega} p^{\omega} v^{\omega}\right) + (1-\lambda)\sum_{\omega\in\Omega} p^{\omega}\left(\sum_{i\in N}\sum_{k\in N} c^{\omega}_{ik} x^{\omega}_{ik} + \theta^{\omega}\right) \tag{62}$$

s.t.: (16), (17), (22), (23), (26), (27)

$$\theta^{\omega} \geq \sum_{i\in N}\sum_{j\in N}\sum_{k\in N}\sigma^{\omega t}_{ijk}x^{\omega}_{ik} + \sum_{i\in N}\sum_{j\in N}\sum_{m\in N}\mu^{\omega t}_{ijm}x^{\omega}_{jm} + \sum_{k\in N}\sum_{m\in N}(h_k + h_m - 1)\delta^{\omega t}_{km} \qquad \forall \omega \in \Omega, t \in T \tag{63}$$

$$\upsilon^{\omega} \geq \sum_{i\in N}\sum_{k\in N} c^{\omega}_{ik}x^{\omega}_{ik} + \theta^{\omega} - \eta \qquad \forall \omega \in \Omega \tag{64}$$

$$\theta^{\omega} \geq 0 \qquad \forall \omega \in \Omega \tag{65}$$

in which T is the set of extreme points for the feasibility region defined by constraints (57)–(58) and (60)–(61). Observe that constraints (16) and (17) assure the installation of at least one hub in the network which in turn guarantees the feasibility of the subproblems at any iteration. Therefore, there is no need for adding feasibility cuts to the MP.

4.1.1. Solving the dual subproblems

An optimal solution for DSP^{ω}_{z} can easily be obtained by inspection as follows:

$$\delta^{\omega *}_{km} = \begin{cases} d_{km}\beta_{\hat{q}^{\omega}_{km}}, & \text{if} \quad \hat{h}_k = \hat{h}_m = 1 \\ 0, & \text{otherwise.} \end{cases} \qquad \forall k, m \in N \tag{66}$$

In order to solve the DSP^{ω}_{y}, we propose a two-phase algorithm that derives the optimal values of dual variables by inspection and without using a standard solver (Ghaffarinasab and Kara, 2019). Our approach for breaking the subproblem into two phases is analogous to the idea of approximating the Pareto optimal cuts (Magnanti and Wong, 1981). In Phase I, we obtain an optimal solution for DSP^{ω}_{y}. Due to the fact that DSP^{ω}_{y} has multiple optimal solutions, in Phase II we choose appropriate values for the optimal dual variables to strengthen the resulting cuts while preserving the optimality and feasibility of the solution.

Phase I. We first note that DSP^{ω}_{y} can be disaggregated into smaller problems, one for each pair (i, j). Moreover, observe that the dual values associated with $\hat{x}^{\omega}_{ik}$ (or $\hat{x}^{\omega}_{jm}$) with zero values do not affect the optimal objective value of the DSP^{ω}_{y}. In other words, whenever $\hat{x}^{\omega}_{ik} = 0$ (or $\hat{x}^{\omega}_{jm} = 0$), we can modify the value of corresponding dual variable without altering the value of objective function, as long as the new values are still feasible (i.e., constraints (57)–(58) are satisfied). Accordingly, we only consider the dual variables σ^{ω}_{ijk} and μ^{ω}_{ijm} corresponding to parameters $\hat{x}^{\omega}_{ik}$ and $\hat{x}^{\omega}_{jm}$ with the values of 1. Note that according to constraint (16), for each node $i \in N$ there is only one hub $k \in N$ under each scenario $\omega \in \Omega$ such that $\hat{x}^{\omega}_{ik} = 1$. Using the notations o_i and o_j for the hubs to which the nodes i and j are assigned, the dual subproblem for each triplet (i, j, ω) can be written as:

$(\textbf{DSP}^{ij\omega}_{y})$

$$\max \ \sigma^{\omega}_{ijo_i} + \mu^{\omega}_{ijo_j} \tag{67}$$

$$\text{s.t.:} \ \sigma^{\omega}_{ijk} + \mu^{\omega}_{ijm} \leq w^{\omega}_{ij}d_{km}\alpha_{\hat{q}^{\omega}_{km}} \qquad \forall k, m \in N \tag{68}$$

$$\sigma^{\omega}_{ijk}, \mu^{\omega}_{ijm} \in \mathbb{R} \qquad \forall k, m \in N \tag{69}$$

Moreover, assume that $\hat{q}^{\omega}_{o_i o_j}$ is the index of the line segment that is applied to the transportation cost on the inter-hub connection (o_i, o_j). It is clear that the optimal objective value of the above model is $w^{\omega}_{ij}d_{o_i o_j}\alpha_{\hat{q}^{\omega}_{o_i o_j}}$, and the corresponding optimal values for variables σ_{ijo_i} and μ_{ijo_j} satisfy the following condition:

$$\sigma^{\omega *}_{ijo_i} + \mu^{\omega *}_{ijo_j} = w^{\omega}_{ij}d_{o_i o_j}\alpha_{\hat{q}^{\omega}_{o_i o_j}} \tag{70}$$

which means that the optimal solution is not unique (i.e., there are multiple optimal solutions). Given any real value κ, the optimal values of $\sigma^{\omega}_{ijo_i}$ and $\mu^{\omega}_{ijo_j}$ can be determined as:

$$\sigma^{\omega *}_{ijo_i} = \kappa \tag{71}$$

$$\mu^{\omega *}_{ijo_j} = w^{\omega}_{ij}d_{o_i o_j}\alpha_{\hat{q}^{\omega}_{o_i o_j}} - \kappa \tag{72}$$

Based on the results of our preliminary experiments, we set the value of κ as $\frac{w^{\omega}_{ij}d_{o_i o_j}\alpha_{\hat{q}^{\omega}_{o_i o_j}}}{2}$ in our computational studies.

Phase II. Once the values of the dual variables $\sigma^{\omega}_{ijo_i}$ and $\mu^{\omega}_{ijo_j}$ are fixed, we now seeks to determine the values of the remaining dual variables in such a way that the resulting Benders cuts be as strong as possible. To this end, for any $m \in N$ such that $m \neq o_j$, we determine the largest possible value for the dual variables μ^{ω}_{ijm} as:

$$\mu^{\omega *}_{ijm} = w^{\omega}_{ij}d_{o_i m}\alpha_{\hat{q}^{\omega}_{o_i m}} - \sigma^{\omega *}_{ijo_i} \tag{73}$$

Furthermore, by fixing the values of μ^{ω}_{ijm}, the largest values of the dual variable σ^{ω}_{ijk}, for all $k \in N$ and $k \neq o_i$, can be calculated as:

$$\sigma^{\omega *}_{ijk} = \min_{m\in N}\{w^{\omega}_{ij}d_{km}\alpha_{\hat{q}^{\omega}_{km}} - \mu^{\omega *}_{ijm}\}. \tag{74}$$

The pseudo-code for the proposed two-phase algorithm is presented in Algorithm 1. The procedure described above enables us to solve DSP^{ω}_{y} and DSP^{ω}_{z} without calling off-the-shelf solvers and obtain strong optimality cuts that significantly reduces the computational burden of the proposed algorithm.

Algorithm 1 : Proposed two-phase procedure for solving DSP_y^{ω}

Input: An instance of the problem and a vector of binary variables $\hat{x}$
for all $\omega \in \Omega$ **do**
  for all $i \in N$ **do**
    for all $j \in N$ **do**
      (Phase I)
      for all $k' \in N$ **do**
        if $\hat{x}^{\omega}_{ik'} = 1$ **then**
          $o_i \leftarrow k'$
        end if
      end for
      for all $m' \in H$ **do**
        if $\hat{x}^{\omega}_{jm'} = 1$ **then**
          $o_j \leftarrow m'$
        end if
      end for
      $\Delta \leftarrow w^{\omega}_{ij} d_{o_i o_j} \alpha_{\hat{q}^{\omega}_{o_i o_j}}$
      $\sigma^{\omega *}_{ijo_i} \leftarrow \frac{\Delta}{2}$
      $\mu^{\omega *}_{ijo_j} \leftarrow \frac{\Delta}{2}$
      (Phase II)
      for all $m \in N, m \neq o_j$ **do**
        $\mu^{\omega *}_{ijm} \leftarrow w^{\omega}_{ij} d_{o_i m} \alpha_{\hat{q}^{\omega}_{o_i m}} - \sigma^{\omega *}_{ijo_i}$
      end for
      for all $k \in N, k \neq o_i$ **do**
        $\sigma^{\omega *}_{ijk} \leftarrow \min_{m \in N} \{ w^{\omega}_{ij} d_{km} \alpha_{\hat{q}^{\omega}_{km}} - \mu^{\omega *}_{ijm} \}$
      end for
    end for
  end for
end for
return $\sigma^{\omega *}_{ijk}, \mu^{\omega *}_{ijm}$ **for all** $i, j, k, m \in N, \omega \in \Omega$.

4.2. Scenario grouping

The size of the proposed MILP formulation increases proportionally to the number of scenarios in our problem which makes it computationally intractable even for moderate number of scenarios. Even the proposed BD algorithm fails to solve the problem to optimality in reasonable time when the number of scenarios is large. Therefore, we need to further enhance our solution procedure to tackle the large instances. To this end, we use the scenario grouping technique, where the original problem is solved separately for a number of groups of scenarios in order to obtain lower and upper bounds on its optimal value. In this approach, instead of solving the problem with the entire set of scenarios, a number of smaller problems are defined based on the subsets of the original set of scenarios. The generated smaller problems are called as group subproblems. We solve the group subproblems using the proposed BD algorithm and obtain a lower bound for the optimal value of original problem by using the optimal values of group subproblems. The optimal solutions of group subproblems are used to obtain a feasible solution to original problem, hence an upper bound. This approach is first proposed by Sandıkçı et al. (2013) for risk-neutral problems. Later, Mahmutoğulları et al. (2018) extend the idea for the risk-averse problems with mean-CVaR objectives.

Let $\mathcal{P} = \{S_j\}_{j=1}^{J}$ be a partition of the set of scenarios Ω, i.e., $\cup_{j=1}^{J} S_j = \Omega$ and $S_j \cap S_{j'} = \emptyset$ for all $j, j' \in \{1, 2, \dots, J\}$ such that $j \neq j'$. A subset of scenarios S_j is called as a *group*. Here, for convenience, we assume that the groups are disjoint, however, the idea can easily be extended to the case where the groups are not disjoint, see Sandıkçı et al. (2013) for details. The probability of scenario $\omega \in S_j$ is adjusted as $\pi^{\omega j} = \frac{p^{\omega}}{\sum_{\omega' \in S_j} p^{\omega'}}$ and the problem with scenario group S_j is solved using these adjusted probabilities.

We call the RASAHLP-FD the *original problem*, and the *group subproblem* $j, (j \in \{1, 2, \dots, J\})$ is defined as in the same structure as the original problem where the sample space Ω is replaced by the group S_j, and the original probability values $p^{\omega}, \omega \in \Omega$ are replaced by the adjusted probabilities $\pi^{\omega j}$ for all $\omega \in S_j$. The optimal values and optimal solutions of the group subproblems are used to obtain lower and upper bounds for the optimal value of the original problem. The details of this approach are provided in Algorithm 2, where we use the presentation of Mahmutoğulları et al. (2019).

Algorithm 2 calculates lower and upper bounds for the original problem. In the lower bounding phase, the group subproblems are solved, and the weighted average of the optimal values of these subproblems is used as a lower bound (Sandıkçı et al., 2013; Mahmutoğulları et al., 2018; Kargar and Mahmutoğulları, 2022). As the number of scenarios in each group subproblem is smaller than the total number of scenarios, we can expect that solving the group subproblems requires less computational effort in comparison with the original problem.

The upper bounding phase constitutes the following steps. After solving each group subproblem j, a vector of first-stage decisions $\boldsymbol{h}_j$ is obtained. If we fix these decisions in the original problem and solve it, the resulting objective function value provides an upper bound for the original problem. We choose the hub set which gives the best upper bound among the solutions obtained by group subproblems.

Algorithm 2 : Proposed scenario grouping algorithm

1: **Input:** An instance of the problem and a partition $\mathcal{P}$ of scenarios
2: $LB \leftarrow -\infty, UB \leftarrow +\infty$
3: Set of all feasible first-stage decisions $\mathcal{H} \leftarrow \{0,1\}^{|N|} \setminus \{(0,0,...,0)\}$
4: Set of evaluated first-stage decisions $D \leftarrow \emptyset$
5: **while** $UB > LB$ **do**
6: **Lower Bounding:**
7: **for all** $j \in \{1,2,...,J\}$ **do**
8: $\mathcal{H} \leftarrow \mathcal{H} \setminus D$
9: Solve the group subproblem j with feasible set $\mathcal{H}$, using the BD algorithm
10: **if** the group subproblem is infeasible **then**
11: **terminate**
12: **else**
13: Let v_j be the optimal objective value of the group subproblem j
14: Let $\boldsymbol{h}_j$ be the optimal first-stage decision of the group subproblem j
15: $D \leftarrow D \cup \{\boldsymbol{h}_j\}$.
16: **end if**
17: **end for**
18: $LB \leftarrow \sum_{j=1}^{J} \pi_j v_j$, where $\pi_j = \sum_{\omega \in S_j} \pi^{\omega j}$
19: **Upper Bounding:**
20: **for all** $\bar{\boldsymbol{h}} \in D$ **do**
21: Solve the original problem with fixed first-stage decision $\bar{\boldsymbol{h}}$
22: Let $\bar{v}$ be the optimal objective value
23: **if** $\bar{v} < UB$ **then**
24: $UB \leftarrow \bar{v}$
25: $\boldsymbol{h}^* \leftarrow \bar{\boldsymbol{h}}$
26: **end if**
27: **end for**
28: **end while**
29: **return** UB and $\boldsymbol{h}^*$.

A key feature of the scenario grouping algorithm is that the set of evaluated first-stage decisions is discarded from the set of feasible solutions (see line 8 in Algorithm 2). Because of the 0–1 nature of the first-stage location decisions h_k, this can be easily accomplished by adding the following integer cuts to the original constraints set of the master problem at each iteration of the scenario grouping algorithm (Ahmed, 2013):

$$\sum_{k \in N | \hat{h}_k = 1} (1 - h_k) + \sum_{k \in N | \hat{h}_k = 0} h_k \geq 1 \qquad \forall \hat{\boldsymbol{h}} \in D \tag{75}$$

in which D denotes the set of evaluated first-stage decisions.

5. Computational experiments

In this section, we describe the conducted computational experiments and present the obtained numerical results to evaluate the performance of proposed solution algorithms and to analyze the effect of different input parameters on optimal solutions. Computational tests were carried out on a computer with Intel(R) Core(TM) i3-3220 CPU of 3.30 GHz and 16 GB of RAM, using the Microsoft Windows 7 operating system. All experiments were executed in sequential form using one thread, and wall-clock times were reported for each case. The proposed solution algorithm was implemented in JAVA, and CPLEX version 12.10 was used for solving the master problem within a branch-and-cut framework employing the lazy constraint callback function available in CPLEX. Cuts were added to the master problem on demand whenever an incumbent integer solution was found. The relative gap parameter of CPLEX was set to 0.003 (i.e., 0.3%) and *MIPEmphasis* parameter value was set to 1 (feasibility) when solving group subproblems using the Benders algorithm in all our experiments.

5.1. Test data

In order to test the efficiency of the proposed models and algorithms, we used a well-known data set from the literature of the HLP, namely the Australia Post (AP) data set first introduced by Ernst and Krishnamoorthy (1996). The AP data set is based on a postal delivery in Sydney, Australia, and consists of 200 nodes representing postal districts. Two types of instances denoted by L (loose) and T (tight) were tested where type T instances present higher hub setup costs for nodes with large flows, while type L instances do not exhibit this feature. In all experiments, the fixed costs were scaled by a factor of 0.75. Using the available code from http://people.brunel.ac.uk/~mastjjb/jeb/orlib/files/phub2.txt, we generated instances with different sizes as $|N| = 10$, 25, 50, and 75 (i.e., with total of 100, 625, 2500, and 5625 commodities, respectively). Since the smaller instances are generated by combining the nodes from the original 200-node data set, the numbering of nodes is not the same in different AP data sets. For example, "node 1" in the AP10 data set is different than "node 1" in the AP25 data set. The weight parameter (λ) was considered at five levels as $\lambda \in \{0, 0.25, 0.5, 0.75, 1\}$ and the value of the risk parameter (γ) was selected as $\gamma \in \{0.7, 0.8, 0.9\}$ for different

Table 1
Characteristics of the employed cost functions.

Interval q	Boundaries $[l_q, u_q)$	Cost function					
		F1		F2		F3	
		α_q	β_q	α_q	β_q	α_q	β_q
1	[0, 50)	1	0	1	0	0.8	0
2	[50, 100)	0.9	5	0.8	10	0.6	10
3	[10, 200)	0.8	15	0.6	30	0.4	30
4	[200, +∞)	0.7	35	0.4	70	0.2	70

Table 2
Comparison of solution times for the AP10 data set.

λ	γ	AP10L						AP10T					
		F1		F2		F3		F1		F2		F3	
		MILP	BD	MILP	BD	MILP	BD	MILP	BD	MILP	BD	MILP	BD
0	–	992.21	6.16	1765.21	3.69	1217.88	2.66	714.88	6.15	833.38	3.15	1282.26	2.40
0.25	0.70	920.83	5.30	1479.64	3.88	1151.02	3.91	1041.31	6.53	1664.97	3.83	750.14	2.74
	0.80	678.28	6.65	1417.27	4.51	2141.89	3.66	847.47	5.78	1469.61	3.49	691.81	2.71
	0.90	1568.19	16.31	2050.24	7.05	3892.03	3.83	644.54	3.88	2378.03	3.36	828.80	2.61
0.5	0.70	1050.62	8.93	1461.87	4.29	2075.92	6.55	1017.22	3.66	1401.70	3.47	937.33	2.70
	0.80	1795.85	9.97	2391.28	8.24	1544.51	7.63	561.15	4.10	1059.00	3.68	997.44	2.87
	0.90	1842.48	11.91	3984.96	14.18	5364.20	13.23	1324.94	8.48	1500.35	6.95	1128.46	2.77
0.75	0.70	1185.55	9.16	2196.52	14.10	2788.46	7.39	803.32	3.68	1454.03	3.87	771.95	2.55
	0.80	1368.85	8.38	3567.83	12.74	2758.11	11.09	528.31	4.54	1593.23	3.90	1088.82	3.11
	0.90	1792.72	14.10	4974.38	17.18	4750.94	13.91	754.71	8.49	2029.20	6.75	967.63	5.50
1	0.70	13629.70	8.53	47845.30	12.72	44897.02	7.22	1980.28	4.50	19041.43	4.30	5954.45	3.18
	0.80	16025.38	12.33	67102.17	12.35	43468.97	13.18	1723.53	8.95	7753.87	7.89	13130.30	3.60
	0.90	44592.86	16.62	111397.87	16.30	85511.67	13.75	5100.62	17.90	68912.82	12.50	39555.74	6.62
Average		6726.42	10.33	19356.50	10.09	15504.82	8.31	1310.94	6.66	8545.51	5.16	5237.32	3.33

problem instances. We generated 50 scenarios for the demand matrix according to Poisson distribution similar to the method used in Rostami et al. (2021), Ghaffarinasab and Kara (2022). Based on this method, under each scenario $\omega \in \Omega$ and for each node $i \in N$, we considered a multiplicative factor r_i^ω denoting the deviation from the base case and which is uniformly distributed between 0.5 and 1.5 (i.e., $r_i^\omega \sim U[0.5, 1.5]$). Then, the demand value for the OD pair (i, j) under scenario ω was generated according to a Poisson random variable with event rate $r_i^\omega r_j^\omega w_{ij}$, in which w_{ij} is the base demand value according to the AP test instance. All the scenarios were assumed to have equal probabilities (i.e., $p^\omega = 0.02$). Each scenario subgroup contained 10 scenarios (i.e., we had five scenario subgroups). Furthermore, we used three different discount functions for reflecting the flow-dependent economies of scale as in Rostami et al. (2022). Each cost function is composed of four line segments and the boundaries, slope, and intercept for each segment are presented in Table 1. The cost function F1 provides a very modest discount as the amount of traffic increases, with the minimum slope being equal to 0.7. The function F2 provides a greater degree of discount, with slopes as low as 0.4, while F3 provides a very aggressive discount scheme, with a minimum slope of 0.2.

5.2. Numerical results

We first analyze the efficiency of the proposed BD algorithm by comparing its solution time with that of solving the monolithic MILP model directly by CPLEX. Table 2 shows the results obtained by solving the RASAHLP-FD with 10-node instances (AP10 data set) using the MILP model (11)–(27) and the proposed BD algorithm. The first row shows the type of solved instances according to their fixed setup cost values, denoted by AP10L and AP10T. The second row presents the type of discount function (F1, F2, or F3). The columns entitled λ and γ denote the weight parameter and the risk parameter, respectively. The columns under the headings "MILP" and "BD" show the solution times (in seconds) for the MILP model and the BD algorithm, respectively.

Comparing the average solution times presented in Table 2, it can be concluded that using the proposed BD algorithm is much computationally efficient that solving the MILP model using CPLEX. While BD is able to solve the instances within small computational times, the solution times for the MILP solver are substantially larger. For example, the average solution time for CPLEX to solve the AP10L instances under cost function F2 is larger than 5 hours, while the same instances are solved within ten seconds using BD. It can also be observed that the instances with loose fixed costs take significantly longer times to be solved compared to the ones with tight fixed costs.

Detailed results obtained by applying the BD algorithm on different problem instances of the AP data set with 10 nodes for both loose and tight fixed costs (i.e., the AP10L and AP10T instances) are reported in Table 3. In addition to optimal objective function values and solution times (denoted by "OF" and "CPU(s)", respectively), we present the optimal set of opened hubs and the number of iterations for the scenario grouping algorithm under the columns labeled as "Hubs" and "# iter", respectively. We also report the

Table 3
Results for the AP10 data set.

Cost Function	λ	γ	AP10L							AP10T						
			OF	Hubs	CPU(s)	# iter	Mean	CVaR	StDev	OF	Hubs	CPU(s)	# iter	Mean	CVaR	StDev
F1	0	0.7	205257.58	1, 4, 5, 7	6.16	2	205257.58	230473.04	22653.85	241355.06	1, 4, 5, 10	6.15	2	241355.06	274175.74	30054.72
		0.8	205257.58	1, 4, 5, 7	6.16	2	205257.58	234888.98	22653.85	241355.06	1, 4, 5, 10	6.15	2	241355.06	280493.35	30054.72
		0.9	205257.58	1, 4, 5, 7	6.16	2	205257.58	243243.82	22653.85	241355.06	1, 4, 5, 10	6.15	2	241355.06	288858.73	30054.72
	0.25	0.7	211561.45	1, 4, 5, 7	5.30	2	205257.58	230473.04	22653.85	249560.23	1, 4, 5, 10	6.53	2	241355.06	274175.74	30054.72
		0.8	212665.43	1, 4, 5, 7	6.65	2	205257.58	234888.98	22653.85	251139.63	1, 4, 5, 10	5.78	2	241355.06	280493.35	30054.72
		0.9	214754.14	1, 4, 5, 7	16.31	4	205257.58	243243.82	22653.85	253230.98	1, 4, 5, 10	3.88	2	241355.06	288858.73	30054.72
	0.5	0.7	217865.31	1, 4, 5, 7	8.93	3	205257.58	230473.04	22653.85	257765.40	1, 4, 5, 10	3.66	2	241355.06	274175.74	30054.72
		0.8	220073.28	1, 4, 5, 7	9.97	3	205257.58	234888.98	22653.85	260924.20	1, 4, 5, 10	4.10	2	241355.06	280493.35	30054.72
		0.9	221688.05	1, 4, 5, 7, 8	11.91	4	208813.01	234563.09	18241.02	265106.89	1, 4, 5, 10	8.48	3	241355.06	288858.73	30054.72
	0.75	0.7	223360.35	1, 4, 5, 7, 8	9.16	3	208813.01	228209.46	18241.02	265970.57	1, 4, 5, 10	3.68	2	241355.06	274175.74	30054.72
		0.8	225917.83	1, 4, 5, 7, 8	8.38	3	208813.01	231619.44	18241.02	270708.77	1, 4, 5, 10	4.54	2	241355.06	280493.35	30054.72
		0.9	228125.57	1, 4, 5, 7, 8	14.10	4	208813.01	234563.09	18241.02	276982.81	1, 4, 5, 10	8.49	3	241355.06	288858.73	30054.72
	1	0.7	228209.46	1, 4, 5, 7, 8	8.53	3	208813.01	228209.46	18241.02	274175.74	1, 4, 5, 10	4.50	2	241355.06	274175.74	30054.72
		0.8	231619.44	1, 4, 5, 7, 8	12.33	4	208813.01	231619.44	18241.02	280493.35	1, 4, 5, 10	8.95	3	241355.06	280493.35	30054.72
		0.9	234563.09	1, 4, 5, 7, 8	16.62	5	208813.01	234563.09	18241.02	288858.73	1, 4, 5, 10	17.90	5	241355.06	288858.73	30054.72
F2	0	0.7	199901.21	3, 4, 7	3.69	2	199901.21	226457.08	25140.74	234430.20	3, 4, 10	3.15	2	234430.20	269304.71	32628.80
		0.8	199901.21	3, 4, 7	3.69	2	199901.21	231188.82	25140.74	234430.20	3, 4, 10	3.15	2	234430.20	275632.70	32628.80
		0.9	199901.21	3, 4, 7	3.69	2	199901.21	233582.76	25140.74	234430.20	3, 4, 10	3.15	2	234430.20	282268.04	32628.80
	0.25	0.7	205967.66	1, 4, 5, 7	3.88	2	200075.74	223643.42	21136.21	243119.97	1, 4, 5, 10	3.83	2	235393.28	266300.04	28190.93
		0.8	207011.65	1, 4, 5, 7	4.51	2	200075.74	227819.36	21136.21	244583.38	1, 4, 5, 10	3.49	2	235393.28	272153.68	28190.93
		0.9	208321.59	3, 4, 7	7.05	3	199901.21	233582.76	25140.74	246389.66	3, 4, 10	3.36	2	234430.20	282268.04	32628.80
	0.5	0.7	211859.58	1, 4, 5, 7	4.29	2	200075.74	223643.42	21136.21	250846.66	1, 4, 5, 10	3.47	2	235393.28	266300.04	28190.93
		0.8	213947.55	1, 4, 5, 7	8.24	3	200075.74	227819.36	21136.21	253773.48	1, 4, 5, 10	3.68	2	235393.28	272153.68	28190.93
		0.9	216741.98	3, 4, 7	14.18	4	199901.21	233582.76	25140.74	257640.11	1, 4, 5, 10	6.95	3	235393.28	279886.94	28190.93
	0.75	0.7	217751.50	1, 4, 5, 7	14.10	4	200075.74	223643.42	21136.21	258573.35	1, 4, 5, 10	3.87	2	235393.28	266300.04	28190.93
		0.8	220883.46	1, 4, 5, 7	12.74	4	200075.74	227819.36	21136.21	262963.58	1, 4, 5, 10	3.90	2	235393.28	272153.68	28190.93
		0.9	223080.86	1, 4, 5, 7, 8	17.18	5	204968.76	229118.23	16953.30	268763.53	1, 4, 5, 10	6.75	3	235393.28	279886.94	28190.93
	1	0.7	223075.11	1, 4, 5, 7, 8	12.72	4	204968.76	223075.11	16953.30	266300.04	1, 4, 5, 10	4.30	2	235393.28	266300.04	28190.93
		0.8	226223.15	1, 4, 5, 7, 8	12.35	4	204968.76	226223.15	16953.30	272153.68	1, 4, 5, 10	7.89	3	235393.28	272153.68	28190.93
		0.9	229118.23	1, 4, 5, 7, 8	16.30	5	204968.76	229118.23	16953.30	279886.94	1, 4, 5, 10	12.50	4	235393.28	279886.94	28190.93
F3	0	0.7	192560.38	1, 4, 5, 7	2.66	2	192560.38	214758.21	19819.80	226924.25	1, 4, 5, 10	2.40	2	226924.25	256351.62	26609.20
		0.8	192560.38	1, 4, 5, 7	2.66	2	192560.38	218840.53	19819.80	226924.25	1, 4, 5, 10	2.40	2	226924.25	261876.81	26609.20
		0.9	192560.38	1, 4, 5, 7	2.66	2	192560.38	226601.16	19819.80	226924.25	1, 4, 5, 10	2.40	2	226924.25	269096.29	26609.20
	0.25	0.7	198109.84	1, 4, 5, 7	3.91	2	192560.38	214758.21	19819.80	234281.09	1, 4, 5, 10	2.74	2	226924.25	256351.62	26609.20
		0.8	199130.42	1, 4, 5, 7	3.66	2	192560.38	218840.53	19819.80	235662.39	1, 4, 5, 10	2.71	2	226924.25	261876.81	26609.20
		0.9	201070.58	1, 4, 5, 7	3.83	2	192560.38	226601.16	19819.80	237467.26	1, 4, 5, 10	2.61	2	226924.25	269096.29	26609.20
	0.5	0.7	203659.29	1, 4, 5, 7	6.55	3	192560.38	214758.21	19819.80	241637.93	1, 4, 5, 10	2.70	2	226924.25	256351.62	26609.20
		0.8	205700.46	1, 4, 5, 7	7.63	3	192560.38	218840.53	19819.80	244400.53	1, 4, 5, 10	2.87	2	226924.25	261876.81	26609.20
		0.9	208072.93	1, 4, 5, 7, 8	13.23	5	196789.26	219356.61	15429.58	248010.27	1, 4, 5, 10	2.77	2	226924.25	269096.29	26609.20
	0.75	0.7	209208.75	1, 4, 5, 7	7.39	3	192560.38	214758.21	19819.80	248994.77	1, 4, 5, 10	2.55	2	226924.25	256351.62	26609.20
		0.8	211459.27	1, 4, 5, 7, 8	11.09	4	196789.26	216349.27	15429.58	253138.67	1, 4, 5, 10	3.11	2	226924.25	261876.81	26609.20
		0.9	213714.77	1, 4, 5, 7, 8	13.91	5	196789.26	219356.61	15429.58	258553.28	1, 4, 5, 10	5.50	3	226924.25	269096.29	26609.20
	1	0.7	213436.04	1, 4, 5, 7, 8	7.22	3	196789.26	213436.04	15429.58	256351.62	1, 4, 5, 10	3.18	2	226924.25	256351.62	26609.20
		0.8	216349.27	1, 4, 5, 7, 8	13.18	5	196789.26	216349.27	15429.58	261876.81	1, 4, 5, 10	3.60	2	226924.25	261876.81	26609.20
		0.9	219356.61	1, 4, 5, 7, 8	13.75	5	196789.26	219356.61	15429.58	269096.29	1, 4, 5, 10	6.62	3	226924.25	269096.29	26609.20
Average					8.86							4.90				

mean and CVaR of total cost in columns labeled as "Mean" and "CVaR", respectively. Since an optimal solution presents different cost values under different scenarios, the standard deviation of these cost values for each instance (using 50 scenarios) is presented under the column labeled as "StDev". Note that when $\lambda = 0$, it is implied that the decision maker is risk-neutral as the whole weight is given to the "mean" component of the objective function, while a larger value for λ such as 0.25, 0.5, 0.75, or 1 assigns a higher weight to the "CVaR" component depending on the level of risk-aversion. Similarly, larger values of γ imply higher level of risk-aversion. We can observe from Table 3 that by increasing the weight parameter λ, the optimal value increases, while the individual components of the objective function (i.e., the mean and CVaR) change in different directions. It needs to be highlighted that, when $\lambda = 0$ we only solve the problem once regardless of the value of γ. Then we calculate the CVaR values based on the set of total cost values corresponding to different scenarios. Therefore, the three lines corresponding to $\lambda = 0$ are the same except for the values presented in CVaR column. As the value of λ increases, the mean value also increases, whereas CVaR decreases. For example, in the AP10L instance with cost function F1 and $\gamma = 0.7$, when $\lambda = 0.5$, the mean and CVaR values are 205257.58 and 230473.04, respectively. However, when λ increases to 0.75, the corresponding values become 208813.01 and 228209.46, respectively. One reason might be the fact that when the value of λ increases, the model puts more focus on the CVaR component and tries to decrease its value which results in solutions that are not optimal from a mean cost perspective. The standard deviation value generally gets smaller by increasing the value of λ. As an example, the standard deviation value is 22653.85 for the AP10L instance with $\lambda = 0.5$ and $\gamma = 0.7$ under cost function F1, whereas the corresponding value decreases to 18241.02 for $\lambda = 0.75$. This shows that when the weight given to CVaR in the objective function increases, the variability of total cost values for different scenarios is reduced.

It is also valuable to study the effect of the risk parameter γ on the objective function components and the standard deviation value. The reported results indicate that by increasing the value of γ, i.e., for higher levels of risk-aversion, the value of CVaR increases as the focus is directed to smaller number of extreme scenarios with the largest realized cost values. Nevertheless, the mean and standard deviation do not show a uniform behavior with respect to the value of γ. While, in general, we observe that the

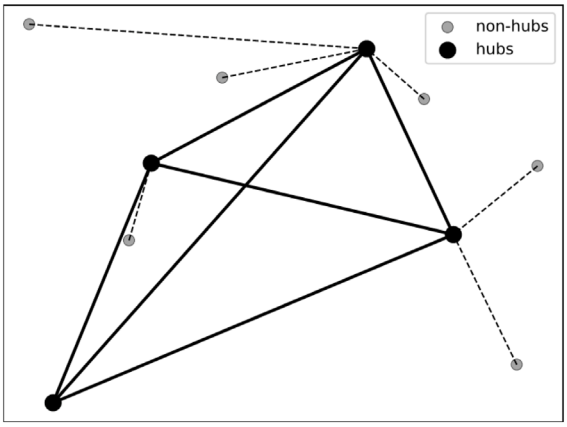

(a) solution for cost function F1

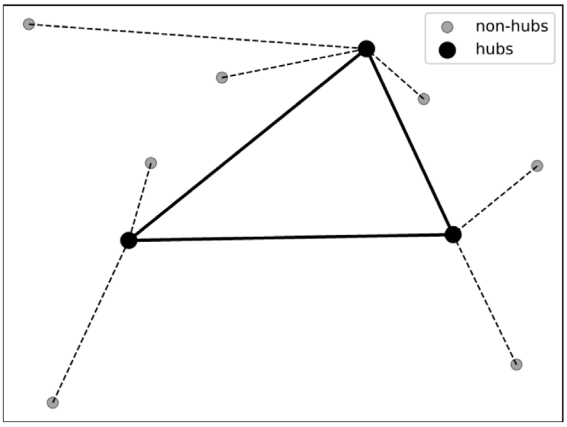

(b) solution for cost function F2

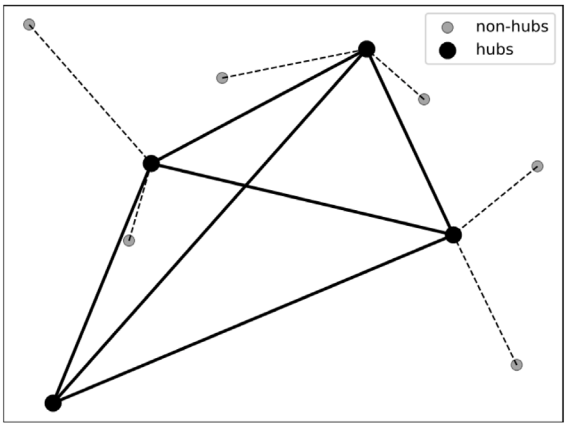

(c) solution for cost function F3

Fig. 2. Changes in the network configuration for different cost functions with the AP10T data set ($\lambda = 0$).

value of mean component increases for larger values of γ, there are some cases that this rule is violated. For example, consider the AP10L instance with F2 and $\lambda = 0.25$. When the value of γ increases from 0.8 to 0.9, the mean cost value decreases from 20075.74 to 199901.21. A similar non-uniform behavior is shown by the standard deviation value. While in general we observe that the value of standard deviation decreases by increasing the values of γ, some exceptions are recorded. In the AP10T instance with F2 and $\lambda = 0.25$, when the value of γ increases from 0.8 to 0.9, the standard deviation value increases from 28190.93 to 32628.80. Indeed, we can observe that in these cases, the solution of risk-averse problem (i.e., $\lambda = 0.25$ and $\gamma = 0.9$) is the same as the solutions of risk-neutral problem (i.e., $\lambda = 0$). Such non-uniform behavior at high values of γ is reported in some other studies in the literature (see Noyan (2012) and Çavuş (2019)).

Regarding the optimal set of located hubs, we can see from Table 3 that hubs 4 and 7 are installed in the optimal solution of every AP10L instance. Also the hubs 1 and 5 are present in 40 of 45 instances (i.e., in almost 90% of cases). For the AP10T instances, it can be observed that in 41 of 45 instances the nodes 1, 4, 5, and 10 are selected as hubs. Only in four instances, i.e., the risk-neutral case ($\lambda = 0$) and the risk-averse instance with $\lambda = 0.25$ and $\gamma = 0.7$ under cost function F2, the optimal sets of hubs include the nodes 3, 4, and 10. It can be concluded that, the risk-averse solutions generally include larger number of opened hubs than the risk-neutral solutions. However, as noted earlier, there are some exceptions in which the hub set for the risk-averse and risk-neutral solutions are identical. Furthermore, by increasing the value of risk parameter γ, the number of opened hubs tend to increase in most cases. For example, consider the AP10L instance with $\lambda = 0.5$ under cost function F1. For the case with $\gamma = 0.7$, the optimal hubs are 1, 4, 5 and 7; but when the value of γ increases to 0.9, an extra hub is opened at node 8.

As far as the flow-dependent cost functions are concerned, it can be observed that optimal objective value is significantly affected by the intensity of the economies of scale. More specifically, the optimal values for the problem instances under cost function F3 are lower than the corresponding instances under cost function F2. Similarly, the optimal values under F2 are smaller than those for cost function F1. The reason is the discount granted for transportation costs under F3 is more intense than the discount for

Table 4
Results for the AP25 data set.

Cost Function	λ	γ	AP25L							AP25T						
			OF	Hubs	CPU(s)	# iter	Mean	CVaR	StDev	OF	Hubs	CPU(s)	# iter	Mean	CVaR	StDev
F1	0	0.7	221057.21	8, 18	149.43	2	221057.21	249799.58	22940.89	274684.98	9, 24	44.00	2	274684.98	312508.62	29930.35
		0.8	221057.21	8, 18	149.43	2	221057.21	256298.62	22940.89	274684.98	9, 24	44.00	2	274684.98	321583.55	29930.35
		0.9	221057.21	8, 18	149.43	2	221057.21	263818.96	22940.89	274684.98	9, 24	44.00	2	274684.98	332699.36	29930.35
	0.25	0.7	228242.81	8, 18	233.64	2	221057.21	249799.58	22940.89	284053.66	8, 24	41.16	2	275336.38	310205.49	27969.89
		0.8	229867.32	8, 14, 18	275.39	2	221596.71	254679.15	21647.05	286161.53	8, 24	39.99	2	275336.38	318636.98	27969.89
		0.9	231569.56	7, 14, 18	247.83	2	222029.37	260190.12	21078.62	288440.76	8, 24	39.79	2	275336.38	327753.90	27969.89
	0.5	0.7	235087.19	7, 14, 18	247.35	2	222029.37	248145.00	21078.62	292770.93	8, 24	43.05	2	275336.38	310205.49	27969.89
		0.8	237940.92	7, 14, 18	477.09	3	222029.37	253852.47	21078.62	296986.68	8, 24	39.84	2	275336.38	318636.98	27969.89
		0.9	241109.75	7, 14, 18	400.07	3	222029.37	260190.12	21078.62	301545.14	8, 24	47.06	2	275336.38	327753.90	27969.89
	0.75	0.7	241616.09	7, 14, 18	259.29	2	222029.37	248145.00	21078.62	301488.21	8, 24	43.26	2	275336.38	310205.49	27969.89
		0.8	245896.69	7, 14, 18	416.38	3	222029.37	253852.47	21078.62	307811.83	8, 24	86.46	3	275336.38	318636.98	27969.89
		0.9	250649.93	7, 14, 18	980.14	5	222029.37	260190.12	21078.62	314649.52	8, 24	101.71	3	275336.38	327753.90	27969.89
	1	0.7	248145.00	7, 14, 18	252.26	2	222029.37	248145.00	21078.62	310205.49	8, 24	53.71	2	275336.38	310205.49	27969.89
		0.8	253852.47	7, 14, 18	840.83	5	222029.37	253852.47	21078.62	318636.98	8, 24	142.36	4	275336.38	318636.98	27969.89
		0.9	260190.12	7, 14, 18	2482.84	12	222029.37	260190.12	21078.62	327753.90	8, 24	173.76	4	275336.38	327753.90	27969.89
F2	0	0.7	215344.44	8, 18	100.12	2	215344.44	242906.33	22002.06	267327.29	9, 24	23.50	2	267327.29	303665.82	28686.81
		0.8	215344.44	8, 18	100.12	2	215344.44	249132.60	22002.06	267327.29	9, 24	23.50	2	267327.29	312301.65	28686.81
		0.9	215344.44	8, 18	100.12	2	215344.44	256310.12	22002.06	267327.29	9, 24	23.50	2	267327.29	323003.99	28686.81
	0.25	0.7	222234.91	8, 18	127.07	2	215344.44	242906.33	22002.06	275849.04	8, 24	23.97	2	267532.43	300798.89	26686.29
		0.8	223663.30	7, 14, 18	130.90	3	216143.00	246224.23	19922.37	277842.55	8, 24	24.58	2	267532.43	308772.92	26686.29
		0.9	225150.29	7, 14, 18	131.78	2	216143.00	252172.15	19922.37	280011.81	8, 24	25.76	2	267532.43	317449.96	26686.29
	0.5	0.7	228490.54	7, 14, 18	145.38	2	216143.00	240838.09	19922.37	284165.66	8, 24	24.81	2	267532.43	300798.89	26686.29
		0.8	231183.61	7, 14, 18	240.60	3	216143.00	246224.23	19922.37	288152.67	8, 24	25.33	2	267532.43	308772.92	26686.29
		0.9	234157.58	7, 14, 18	380.57	4	216143.00	252172.15	19922.37	292491.19	8, 24	26.94	2	267532.43	317449.96	26686.29
	0.75	0.7	234664.32	7, 14, 18	162.37	2	216143.00	240838.09	19922.37	292482.27	8, 24	26.01	2	267532.43	300798.89	26686.29
		0.8	238703.92	7, 14, 18	387.52	4	216143.00	246224.23	19922.37	298462.80	8, 24	46.11	3	267532.43	308772.92	26686.29
		0.9	243164.86	7, 14, 18	571.64	5	216143.00	252172.15	19922.37	304970.58	8, 24	53.40	3	267532.43	317449.96	26686.29
	1	0.7	240838.09	7, 14, 18	289.54	3	216143.00	240838.09	19922.37	300798.89	8, 24	32.93	2	267532.43	300798.89	26686.29
		0.8	246224.23	7, 14, 18	673.12	5	216143.00	246224.23	19922.37	308772.92	8, 24	88.86	4	267532.43	308772.92	26686.29
		0.9	252172.15	7, 14, 18	1595.65	10	216143.00	252172.15	19922.37	317449.96	8, 24	78.95	3	267532.43	317449.96	26686.29
F3	0	0.7	210167.28	7, 14, 18	64.60	2	210167.28	233866.64	19120.03	261197.99	8, 24	15.90	2	261197.99	293348.70	25770.76
		0.8	210167.28	7, 14, 18	64.60	2	210167.28	239007.93	19120.03	261197.99	8, 24	15.90	2	261197.99	301000.75	25770.76
		0.9	210167.28	7, 14, 18	64.60	2	210167.28	244733.05	19120.03	261197.99	8, 24	15.90	2	261197.99	309384.08	25770.76
	0.25	0.7	216092.12	7, 14, 18	66.26	2	210167.28	233866.64	19120.03	269235.67	8, 24	16.77	2	261197.99	293348.70	25770.76
		0.8	217377.44	7, 14, 18	72.24	2	210167.28	239007.93	19120.03	271148.68	8, 24	18.02	2	261197.99	301000.75	25770.76
		0.9	218808.72	7, 14, 18	127.68	3	210167.28	244733.05	19120.03	273244.51	8, 24	19.03	2	261197.99	309384.08	25770.76
	0.5	0.7	222016.96	7, 14, 18	83.68	2	210167.28	233866.64	19120.03	277273.35	8, 24	18.19	2	261197.99	293348.70	25770.76
		0.8	224587.60	7, 14, 18	162.62	3	210167.28	239007.93	19120.03	281099.37	8, 24	31.37	2	261197.99	301000.75	25770.76
		0.9	227450.17	7, 14, 18	214.92	4	210167.28	244733.05	19120.03	285291.03	8, 24	18.94	2	261197.99	309384.08	25770.76
	0.75	0.7	227941.80	7, 14, 18	148.54	3	210167.28	233866.64	19120.03	285311.02	8, 24	17.74	2	261197.99	293348.70	25770.76
		0.8	231797.76	7, 14, 18	256.80	4	210167.28	239007.93	19120.03	291050.06	8, 24	31.35	3	261197.99	301000.75	25770.76
		0.9	236091.61	7, 14, 18	633.27	7	210167.28	244733.05	19120.03	297337.55	8, 24	20.45	2	261197.99	309384.08	25770.76
	1	0.7	233866.64	7, 14, 18	297.18	4	210167.28	233866.64	19120.03	293348.70	8, 24	41.25	3	261197.99	293348.70	25770.76
		0.8	239007.93	7, 14, 18	571.87	6	210167.28	239007.93	19120.03	301000.75	8, 24	42.45	3	261197.99	301000.75	25770.76
		0.9	244733.05	7, 14, 18	1855.21	14	210167.28	244733.05	19120.03	309384.08	8, 24	102.25	5	261197.99	309384.08	25770.76
Average					386.27							43.51				

F2; and the discount under F2 is in turn more intense than the discount under F1. The results presented in Table 3 also show that the optimal hubs are remarkably stable with respect to the type of cost function. For instance, the optimal hubs for all the cases under cost function F1 are the same as those of the corresponding cases under cost function F3 for the AP10T data set. However, detailed analysis reveals that the network configuration (including the location of hubs, inter-hub and spoke links) are different for some instances. For example, we illustrate the optimal network for the risk-neutral problem ($\lambda = 0$) with the AP10T data set for the three cost functions in Fig. 2. The hubs are shown as large black circles and the non-hub nodes as small gray circles. The inter-hub connections are depicted by using thick lines and the spoke links are shown and thin dashed lines. Since the spoke links (i.e., the allocation decisions) depend on random scenarios, we depict the spoke links corresponding to first scenario. As can be seen, the optimal network takes different configurations under different cost functions. Note that, although the networks for F1 and F3, look very similar, the allocation of one non-hub node (the node at the upper left corner) is different in the two solutions.

Table 4 presents the results by solving the problem with the AP25 data set. The solution times show that the instances with 25 nodes are generally solved within quite short computational times. While the AP25L instances are solved in an average time of less than 7 min, the average solution time for the AP25T instances is less than one minute. We can also observe that the time for solving risk-averse problems (i.e., the instances with $\lambda > 0$ or the ones with large γ values) is in general greater than the solution time for risk-neutral case. The reason is that for the risk-averse problems, the number of iterations of the scenario grouping algorithm is larger than the iteration number of risk-neutral instances.

We can observe from Table 4 that the number of opened hubs in the instances with tight setup costs (AP25T) is in general larger than the number of hubs for the instances with loose setup costs (AP25L) as the tight fixed setup costs are larger than loose ones. Note that the variability in the set of optimal hubs is more noticeable in the instances with loose setup costs. It is also interesting to analyze the effect of considering risk on the optimal network configuration. We depict the optimal network configuration for the AP25L instance with cost function F1 both for risk-neutral and risk-averse cases in Fig. 3. Each subfigure shows the location of

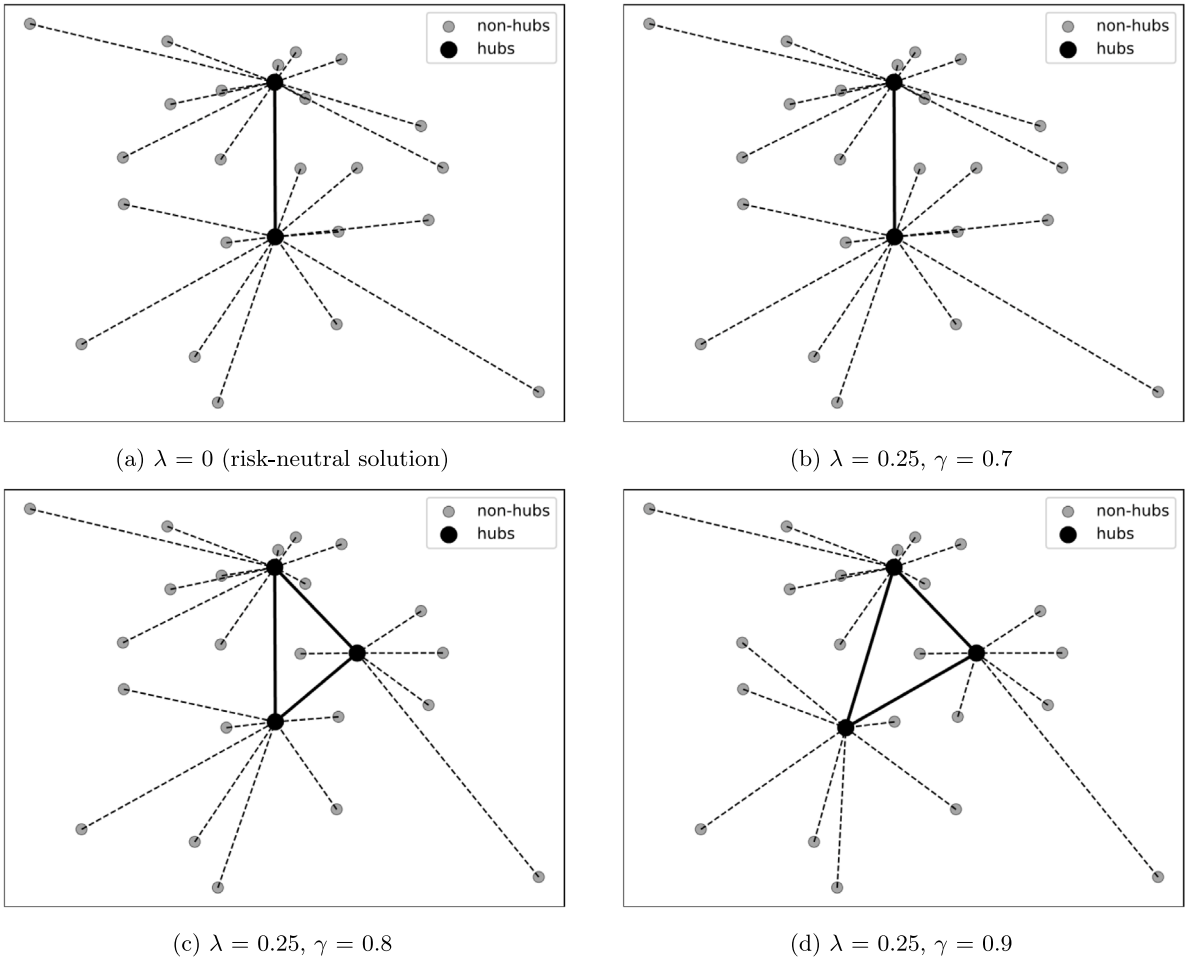

(a) $\lambda = 0$ (risk-neutral solution) (b) $\lambda = 0.25, \gamma = 0.7$

(c) $\lambda = 0.25, \gamma = 0.8$ (d) $\lambda = 0.25, \gamma = 0.9$

Fig. 3. Changes in the network configuration with respect to risk-aversion for the AP25L data with cost function F1.

installed hubs, inter-hub connections, and the allocation from the non-hub nodes to the hubs corresponding to the first scenario. Fig. 3(a) shows the risk-neutral solution (i.e., $\lambda = 0$), whereas Figs. 3(b–d) present the risk-averse solutions with $\lambda = 0.25$ for different values of the risk parameter γ. As can be seen, the optimal network configuration changes as the level of risk-aversion increases.

Results for solving the problem with the AP50 data set are presented in Table 5. We observe similar patterns regarding the number of opened hubs and variation in solution time to those we saw in the previous tables. However, we can notice a stable set of optimal hub locations for instances with tight fixed costs. This might be due to larger values of the tight fixed costs (compared their corresponding loose values) which makes the model select smaller number of hubs, usually including the nodes with high inbound/outbound traffic volume or the ones located at central locations. In this case, two hubs are located at nodes 17 and 48 which are positioned at relatively central locations among the set of all nodes. It should be noted that this type of stability in location of hubs is observed in other risk-averse hub location problems (see for example (Ghaffarinasab and Kara, 2022)).

Note that the average time required for solving the AP50T instances is substantially smaller than that of the AP50L instances. One reason for this difference is that the number of iterations for the scenario grouping algorithm is smaller for the instances with tight fixed costs as compared that of the instances with loose fixed costs. Reported solution times show the efficiency of the proposed procedure in solving real-life problems with large number of nodes and scenarios.

We can observe from Tables 3–5 that the solution times grow exponentially by increasing the number of nodes in the network. The number of scenarios is another factor that impacts the solution time as it affects the size of the model in terms of number of decision variables and constraints. Therefore, to tackle larger instances (in terms of number of nodes) of the problem, one way is to reduce the number of scenarios. The results for solving the AP75 data set with 30 scenarios (three scenario groups, each including 10 scenarios) are presented in Table 6.

As can be seen from Table 6, the average solution times are comparable to those of the AP50 data set due to reduced number of scenarios. It should also be noted that the diversity of the scenarios (affected by the method used for generating them) can influence the solution times. In other words, if the scenarios are more different from each other, it is expected that the problem

Table 5
Results for the AP50 data set.

Cost Function	λ	γ	AP50L							AP50T						
			OF	Hubs	CPU(s)	# iter	Mean	CVaR	StDev	OF	Hubs	CPU(s)	# iter	Mean	CVaR	StDev
F1	0	0.7	226214.01	15, 36	5036.37	2	226214.01	247983.34	18061.50	280933.33	17, 48	223.14	1	280933.33	306111.60	20971.38
		0.8	226214.01	15, 36	5036.37	2	226214.01	251883.29	18061.50	280933.33	17, 48	223.14	1	280933.33	310802.40	20971.38
		0.9	226214.01	15, 36	5036.37	2	226214.01	257298.20	18061.50	280933.33	17, 48	223.14	1	280933.33	315123.45	20971.38
	0.25	0.7	231628.08	15, 27, 35	5551.22	2	226774.88	246187.68	16315.90	287227.90	17, 48	354.63	2	280933.33	306111.60	20971.38
		0.8	232501.65	15, 27, 35	6729.01	2	226774.88	249681.97	16315.90	288400.60	17, 48	319.03	2	280933.33	310802.40	20971.38
		0.9	233666.42	15, 27, 35	7166.35	2	226774.88	254341.05	16315.90	289480.86	17, 48	323.58	2	280933.33	315123.45	20971.38
	0.5	0.7	236481.28	15, 27, 35	5427.63	2	226774.88	246187.68	16315.90	293522.46	17, 48	332.32	2	280933.33	306111.60	20971.38
		0.8	238228.43	15, 27, 35	6591.31	2	226774.88	249681.97	16315.90	295867.86	17, 48	347.61	2	280933.33	310802.40	20971.38
		0.9	240557.97	15, 27, 35	12869.79	3	226774.88	254341.05	16315.90	298028.39	17, 48	348.84	2	280933.33	315123.45	20971.38
	0.75	0.7	241334.48	15, 27, 35	11092.15	3	226774.88	246187.68	16315.90	299817.03	17, 48	321.40	2	280933.33	306111.60	20971.38
		0.8	243955.20	15, 27, 35	7633.17	2	226774.88	249681.97	16315.90	303335.13	17, 48	362.90	2	280933.33	310802.40	20971.38
		0.9	247449.51	15, 27, 35	14825.26	3	226774.88	254341.05	16315.90	306575.92	17, 48	324.53	2	280933.33	315123.45	20971.38
	1	0.7	246187.68	15, 27, 35	16422.48	3	226774.88	246187.68	16315.90	306111.60	17, 48	377.64	2	280933.33	306111.60	20971.38
		0.8	249681.97	15, 27, 35	16038.49	3	226774.88	249681.97	16315.90	310802.40	17, 48	424.06	2	280933.33	310802.40	20971.38
		0.9	254158.97	6, 27, 35	18663.77	3	228417.92	254158.97	15695.54	315123.45	17, 48	553.10	2	280933.33	315123.45	20971.38
F2	0	0.7	220434.20	15, 35	11321.58	2	220434.20	240470.45	16723.31	274277.25	17, 48	53.53	1	274277.25	298443.21	20142.81
		0.8	220434.20	15, 35	11321.58	2	220434.20	244052.58	16723.31	274277.25	17, 48	53.53	1	274277.25	302968.40	20142.81
		0.9	220434.20	15, 35	11321.58	2	220434.20	248934.19	16723.31	274277.25	17, 48	53.53	1	274277.25	307149.79	20142.81
	0.25	0.7	225443.27	15, 35	3333.56	3	220434.20	240470.45	16723.31	280318.74	17, 48	103.36	2	274277.25	298443.21	20142.81
		0.8	226338.80	15, 35	2286.41	2	220434.20	244052.58	16723.31	281450.04	17, 48	106.18	2	274277.25	302968.40	20142.81
		0.9	227559.20	15, 35	4096.32	3	220434.20	248934.19	16723.31	282495.39	17, 48	104.20	2	274277.25	307149.79	20142.81
	0.5	0.7	230371.38	15, 27, 35	5467.19	3	221205.46	239537.29	15478.29	286360.23	17, 48	105.76	2	274277.25	298443.21	20142.81
		0.8	232058.89	15, 27, 35	5766.66	3	221205.46	242912.31	15478.29	288622.83	17, 48	103.39	2	274277.25	302968.40	20142.81
		0.9	234143.01	3, 27, 35	7126.45	3	222081.62	246204.41	14891.08	290713.52	17, 48	101.80	2	274277.25	307149.79	20142.81
	0.75	0.7	234954.33	15, 27, 35	5434.84	3	221205.46	239537.29	15478.29	292401.72	17, 48	98.69	2	274277.25	298443.21	20142.81
		0.8	237485.60	15, 27, 35	6016.81	3	221205.46	242912.31	15478.29	295795.61	17, 48	125.45	2	274277.25	302968.40	20142.81
		0.9	240173.71	3, 27, 35	7799.76	3	222081.62	246204.41	14891.08	298931.65	17, 48	136.83	2	274277.25	307149.79	20142.81
	1	0.7	239537.29	15, 27, 35	6590.04	3	221205.46	239537.29	15478.29	298443.21	17, 48	189.96	2	274277.25	298443.21	20142.81
		0.8	242912.31	15, 27, 35	7577.42	3	221205.46	242912.31	15478.29	302968.40	17, 48	195.97	2	274277.25	302968.40	20142.81
		0.9	246204.41	3, 27, 35	11115.24	3	222081.62	246204.41	14891.08	307149.79	17, 48	284.86	2	274277.25	307149.79	20142.81
F3	0	0.7	214910.03	3, 27, 35	1292.01	3	214910.03	231802.26	14141.86	268468.21	17, 48	64.80	2	268468.21	291896.61	19556.53
		0.8	214910.03	3, 27, 35	1292.01	3	214910.03	234918.48	14141.86	268468.21	17, 48	64.80	2	268468.21	296289.53	19556.53
		0.9	214910.03	3, 27, 35	1292.01	3	214910.03	237970.88	14141.86	268468.21	17, 48	64.80	2	268468.21	300346.24	19556.53
	0.25	0.7	219133.09	3, 27, 35	1673.91	3	214910.03	231802.26	14141.86	274325.31	17, 48	73.20	2	268468.21	291896.61	19556.53
		0.8	219912.14	3, 27, 35	911.56	2	214910.03	234918.48	14141.86	275423.54	17, 48	80.07	2	268468.21	296289.53	19556.53
		0.9	220675.24	3, 27, 35	993.76	2	214910.03	237970.88	14141.86	276437.72	17, 48	76.09	2	268468.21	300346.24	19556.53
	0.5	0.7	223356.15	3, 27, 35	1072.71	2	214910.03	231802.26	14141.86	280182.41	17, 48	83.81	2	268468.21	291896.61	19556.53
		0.8	224914.26	3, 27, 35	1038.34	2	214910.03	234918.48	14141.86	282378.87	17, 48	75.17	2	268468.21	296289.53	19556.53
		0.9	226440.45	3, 27, 35	1513.40	2	214910.03	237970.88	14141.86	284407.23	17, 48	60.22	2	268468.21	300346.24	19556.53
	0.75	0.7	227579.21	3, 27, 35	1720.30	3	214910.03	231802.26	14141.86	286039.51	17, 48	62.52	2	268468.21	291896.61	19556.53
		0.8	229916.37	3, 27, 35	1275.19	2	214910.03	234918.48	14141.86	289334.20	17, 48	66.87	2	268468.21	296289.53	19556.53
		0.9	232205.67	3, 27, 35	2737.11	3	214910.03	237970.88	14141.86	292376.74	17, 48	94.34	2	268468.21	300346.24	19556.53
	1	0.7	231802.26	3, 27, 35	3497.77	3	214910.03	231802.26	14141.86	291896.61	17, 48	105.86	2	268468.21	291896.61	19556.53
		0.8	234918.48	3, 27, 35	3833.69	3	214910.03	234918.48	14141.86	296289.53	17, 48	111.49	2	268468.21	296289.53	19556.53
		0.9	237970.88	3, 27, 35	4574.57	3	214910.03	237970.88	14141.86	300346.24	17, 48	133.85	2	268468.21	300346.24	19556.53
Average					6209.19							179.87				

will become harder, and thus require longer time to be solved. Such an observation is reported in Mahmutoğulları et al. (2019) for some risk-averse stochastic programming problem.

5.3. Effect of flow-dependent economies of scale on optimal solutions

As stated earlier, using flow-dependent economies of scale in modeling the transportation costs is one of the extensions in this paper, which makes the problem more computationally challenging compared to the classical hub location problem with flow-independent discount scheme. In this section, we focus on a comparison analysis to highlight the differences between the optimal solutions of the problem under both discount schemes in terms of network structure. To do this, we solved the problem in its classical setting by applying a fixed discount factor α to inter-hub transportation costs. To have a fair comparison, we set the value of discount factor equal to average of the four line segments for each cost function (i.e., 0.85, 0.7, and 0.5 for F1, F2, and F3, respectively). The results for solving the problem with AP25 data set including the optimal value and the optimal set of opened hubs are presented in Table 7.

Comparing the results presented in Table 7 with those reported in Table 4, it can be seen that in 18 instances solved from the AP25 data set, the optimal set of hubs differ from that of the problem with flow-dependent discount. In 13 out of these 18 cases, the number of hubs opened under the classical discount exceeds by one the number of hubs opened under flow-dependent discount. In the remaining five cases, the number of opened hubs is the same but their compositions differ. For example, the optimal network configurations for the flow-dependent and fixed discount schemes for the AP25L instance with cost function F2, $\lambda = 0.75$, and $\gamma = 0.8$ are presented in Fig. 4. Since the spoke links (i.e., the allocation decisions) depend on random scenarios, we depict the spoke

Table 6
Results for the AP75 data set ($|\Omega| = 30$).

Cost Function	λ	γ	AP75L							AP75T						
			OF	Hubs	CPU(s)	# iter	Mean	CVaR	StDev	OF	Hubs	CPU(s)	# iter	Mean	CVaR	StDev
F1	0	0.7	116275.06	21, 52	6848.55	2	116275.06	131352.92	12722.99	150939.48	48	366.03	2	150939.48	178856.49	23351.40
		0.8	116275.06	21, 52	6848.55	2	116275.06	135855.07	12722.99	150939.48	48	366.03	2	150939.48	186259.80	23351.40
		0.9	116275.06	21, 52	6848.55	2	116275.06	141817.78	12722.99	150939.48	48	366.03	2	150939.48	197508.02	23351.40
	0.25	0.7	120044.52	21, 52	6272.00	2	116275.06	131352.92	12722.99	157918.73	48	395.50	2	150939.48	178856.49	23351.40
		0.8	121114.37	8, 52	5559.56	2	116275.64	135630.54	12648.13	159409.39	22, 48	463.55	2	151607.23	182815.87	20497.76
		0.9	122443.86	8, 52	4241.70	2	116275.64	140948.49	12648.13	161660.88	22, 48	496.71	3	151607.23	191821.80	20497.76
	0.5	0.7	123813.99	21, 52	5863.10	2	116275.06	131352.92	12722.99	164467.39	22, 48	379.88	2	151607.23	177327.54	20497.76
		0.8	125953.09	8, 52	11931.30	3	116275.64	135630.54	12648.13	167211.55	22, 48	270.15	2	151607.23	182815.87	20497.76
		0.9	128612.07	8, 52	10757.13	3	116275.64	140948.49	12648.13	171714.52	22, 48	232.30	2	151607.23	191821.80	20497.76
	0.75	0.7	127583.46	21, 52	6305.79	2	116275.06	131352.92	12722.99	170897.47	22, 48	450.16	3	151607.23	177327.54	20497.76
		0.8	130791.82	8, 52	11581.91	3	116275.64	135630.54	12648.13	175013.71	22, 48	250.94	2	151607.23	182815.87	20497.76
		0.9	134780.28	8, 52	10402.32	3	116275.64	140948.49	12648.13	181768.16	22, 48	284.04	2	151607.23	191821.80	20497.76
	1	0.7	131352.92	21, 52	8369.19	2	116275.06	131352.92	12722.99	177327.54	22, 48	407.80	2	151607.23	177327.54	20497.76
		0.8	135630.54	8, 52	10225.44	2	116275.64	135630.54	12648.13	182815.87	22, 48	295.10	2	151607.23	182815.87	20497.76
		0.9	140948.49	8, 52	24502.80	3	116275.64	140948.49	12648.13	191821.80	22, 48	640.62	3	151607.23	191821.80	20497.76
F2	0	0.7	114463.14	8, 52	4181.45	2	114463.14	128787.07	11907.56	149763.23	22, 48	72.73	1	149763.23	174687.73	19897.65
		0.8	114463.14	8, 52	4181.45	2	114463.14	132634.05	11907.56	149763.23	22, 48	72.73	1	149763.23	179990.91	19897.65
		0.9	114463.14	8, 52	4181.45	2	114463.14	137579.09	11907.56	149763.23	22, 48	72.73	1	149763.23	188779.54	19897.65
	0.25	0.7	118044.12	8, 52	4726.02	2	114463.14	128787.07	11907.56	155994.35	22, 48	211.61	2	149763.23	174687.73	19897.65
		0.8	119005.87	8, 52	3582.57	2	114463.14	132634.05	11907.56	157320.15	22, 48	177.44	2	149763.23	179990.91	19897.65
		0.9	120242.13	8, 52	2916.72	2	114463.14	137579.09	11907.56	159517.30	22, 48	168.48	2	149763.23	188779.54	19897.65
	0.5	0.7	121594.42	21, 52	3446.39	2	114495.31	128693.54	12024.08	162225.48	22, 48	173.87	2	149763.23	174687.73	19897.65
		0.8	123548.60	8, 52	5312.36	3	114463.14	132634.05	11907.56	164877.07	22, 48	200.36	2	149763.23	179990.91	19897.65
		0.9	126021.12	8, 52	5277.06	3	114463.14	137579.09	11907.56	169271.38	22, 48	160.95	2	149763.23	188779.54	19897.65
	0.75	0.7	125143.98	21, 52	4849.28	2	114495.31	128693.54	12024.08	168456.60	22, 48	177.44	2	149763.23	174687.73	19897.65
		0.8	128091.32	8, 52	3969.36	2	114463.14	132634.05	11907.56	172433.99	22, 48	225.76	2	149763.23	179990.91	19897.65
		0.9	131800.11	8, 52	6518.69	3	114463.14	137579.09	11907.56	179025.46	22, 48	236.24	2	149763.23	188779.54	19897.65
	1	0.7	128693.54	21, 52	6335.55	2	114495.31	128693.54	12024.08	174687.73	22, 48	319.03	2	149763.23	174687.73	19897.65
		0.8	132634.05	8, 52	8107.29	2	114463.14	132634.05	11907.56	179990.91	22, 48	225.14	2	149763.23	179990.91	19897.65
		0.9	137579.09	8, 52	11846.66	3	114463.14	137579.09	11907.56	188779.54	22, 48	524.57	3	149763.23	188779.54	19897.65
F3	0	0.7	111975.38	8, 52	2892.42	2	111975.38	125531.08	11319.03	147808.03	22, 48	53.68	1	147808.03	172161.80	19468.43
		0.8	111975.38	8, 52	2892.42	2	111975.38	129223.29	11319.03	147808.03	22, 48	53.68	1	147808.03	177360.75	19468.43
		0.9	111975.38	8, 52	2892.42	2	111975.38	133918.85	11319.03	147808.03	22, 48	53.68	1	147808.03	186020.87	19468.43
	0.25	0.7	115364.31	8, 52	2088.89	2	111975.38	125531.08	11319.03	153896.47	22, 48	150.40	2	147808.03	172161.80	19468.43
		0.8	116287.36	8, 52	2224.14	2	111975.38	129223.29	11319.03	155196.21	22, 48	147.47	2	147808.03	177360.75	19468.43
		0.9	117461.25	8, 52	2321.81	2	111975.38	133918.85	11319.03	157361.24	22, 48	178.11	2	147808.03	186020.87	19468.43
	0.5	0.7	118753.23	8, 52	2012.84	2	111975.38	125531.08	11319.03	159984.92	22, 48	149.01	2	147808.03	172161.80	19468.43
		0.8	120599.33	8, 52	1839.93	2	111975.38	129223.29	11319.03	162584.39	22, 48	132.72	2	147808.03	177360.75	19468.43
		0.9	122947.11	8, 52	2119.73	2	111975.38	133918.85	11319.03	166914.45	22, 48	124.69	2	147808.03	186020.87	19468.43
	0.75	0.7	122142.15	8, 52	2135.09	2	111975.38	125531.08	11319.03	166073.36	22, 48	128.56	2	147808.03	172161.80	19468.43
		0.8	124911.31	8, 52	1950.69	2	111975.38	129223.29	11319.03	169972.57	22, 48	163.06	2	147808.03	177360.75	19468.43
		0.9	128432.98	8, 52	1965.02	2	111975.38	133918.85	11319.03	176467.66	22, 48	199.74	2	147808.03	186020.87	19468.43
	1	0.7	125531.08	8, 52	4211.18	2	111975.38	125531.08	11319.03	172161.80	22, 48	283.44	2	147808.03	172161.80	19468.43
		0.8	129223.29	8, 52	6094.34	3	111975.38	129223.29	11319.03	177360.75	22, 48	271.15	2	147808.03	177360.75	19468.43
		0.9	133918.85	8, 52	4177.08	2	111975.38	133918.85	11319.03	185355.70	22, 67	204.97	2	155163.54	185355.70	14879.70
Average					5729.07							243.96				

links corresponding to first scenario. As can be seen, the network configuration in terms of the location of hubs and the established linkages can be different from the case in which the fixed discount setting is used.

5.4. Managerial insights

The results obtained by our computational experiments highlight some managerial insights, which can be useful for the practitioners and researchers in the optimal design of risk-averse hub networks:

- Considering risk is an important issue in the design of hub networks. Due to underlying uncertainties in the problem parameters, ignoring risk can lead to solutions with quite diverse total cost values under different scenarios, which is not desirable from a risk-averse decision maker's perspective. Risk-averse hub location provides the decision makers with a solution, which is more predictable in terms of random total cost compared to the risk-neutral case. Moreover, risk-averse hub location results in solutions with a different network configuration in comparison with the risk-neutral problem. As seen in Fig. 3, the optimal network configuration changes (both in terms of location of hubs and allocation of non-hub nodes to the hubs) as the level of risk-aversion increases. Also, as risk-aversion increases, more hubs are opened in order to decrease the cost of extreme situations with large demand by utilizing the discount between hub flows.
- There is a trade-off between the network's efficiency and risk-aversion. As the level of risk-aversion (represented by the parameters λ and γ) increases, the efficiency of the hub network slightly decreases, resulting in slightly larger system costs. The expected cost incurred by the decision maker increases in order to decrease the dispersion of random cost as risk-aversion increases. As seen in Tables 3–6, when the risk-neutral results are baseline, the percentage increase in total cost is much less than the percentage decrease in dispersion. For instance, when $\lambda = 1$ and $\gamma = 0.9$ (i.e. the most risk-averse case) in the test instance AP25T with cost function F1, the percentage loss in expected total cost (i.e. mean) is 0.24% while the percentage

Table 7
Results for the AP25 data set with fixed (flow-independent) discount.

α	λ	γ	AP25L		AP25T	
			OF	Hubs	OF	Hubs
0.85	0	0.7	222945.78	8, 14, 18	277684.42	9, 24
		0.8	222945.78	8, 14, 18	277684.42	9, 24
		0.9	222945.78	8, 14, 18	277684.42	9, 24
	0.25	0.7	229929.91	8, 14, 18	287325.97	9, 24
		0.8	231414.32	8, 14, 18	289588.64	8, 24
		0.9	233203.12	8, 14, 18	291920.95	8, 24
	0.5	0.7	236827.10	7, 14, 18	296347.20	8, 24
		0.8	239779.67	7, 14, 18	300676.36	8, 24
		0.9	243016.88	7, 14, 18	305340.97	8, 24
	0.75	0.7	243527.64	7, 14, 18	305270.35	8, 24
		0.8	247956.50	7, 14, 18	311764.08	8, 24
		0.9	252812.32	7, 14, 18	318760.99	8, 24
	1	0.7	250228.18	7, 14, 18	314193.49	8, 24
		0.8	256133.33	7, 14, 18	322851.80	8, 24
		0.9	262607.76	7, 14, 18	332181.02	8, 24
0.7	0	0.7	218997.35	8, 14, 18	273326.17	9, 24
		0.8	218997.35	8, 14, 18	273326.17	9, 24
		0.9	218997.35	8, 14, 18	273326.17	9, 24
	0.25	0.7	225577.11	7, 14, 18	282679.57	8, 24
		0.8	226998.46	7, 14, 18	284787.44	8, 24
		0.9	228585.47	7, 14, 18	287066.67	8, 24
	0.5	0.7	232096.39	7, 14, 18	291396.85	8, 24
		0.8	234939.10	7, 14, 18	295612.59	8, 24
		0.9	238113.12	7, 14, 18	300171.05	8, 24
	0.75	0.7	238615.67	7, 14, 18	300114.12	8, 24
		0.8	242879.73	7, 14, 18	306437.74	8, 24
		0.9	247640.77	7, 14, 18	313275.43	8, 24
	1	0.7	245134.96	7, 14, 18	308831.40	8, 24
		0.8	250820.37	7, 14, 18	317262.89	8, 24
		0.9	256547.55	2, 8, 14, 18	326379.81	8, 24
0.5	0	0.7	213152.34	7, 14, 18	267515.16	9, 24
		0.8	213152.34	7, 14, 18	267515.16	9, 24
		0.9	213152.34	7, 14, 18	267515.16	9, 24
	0.25	0.7	219428.75	7, 14, 18	276323.81	8, 24
		0.8	220791.10	7, 14, 18	278355.64	8, 24
		0.9	222316.42	7, 14, 18	280562.82	8, 24
	0.5	0.7	225705.16	7, 14, 18	284775.38	8, 24
		0.8	228429.86	7, 14, 18	288839.05	8, 24
		0.9	231480.49	7, 14, 18	293253.40	8, 24
	0.75	0.7	231981.57	7, 14, 18	293226.95	8, 24
		0.8	236060.82	2, 8, 15, 18	299322.45	8, 24
		0.9	239514.18	2, 8, 15, 18	305943.98	8, 24
	1	0.7	238257.98	7, 14, 18	301678.52	8, 24
		0.8	242599.46	2, 8, 15, 18	309805.86	8, 24
		0.9	247203.94	2, 8, 15, 18	318634.56	8, 24

gain in standard deviation of total cost (i.e. StDev) and CVaR of total cost is 6.55% and 1.49%, respectively. The risk-aversion provides a more predictable environment for the decision makers by decreasing the dispersion of total cost while not decreasing the expected total cost significantly.

- The type of employed discount function affects the optimal solution of the problem in terms of the objective function value and the network configuration. As can be seen from Fig. 2, the optimal set of opened hubs and the allocation of non-hub nodes to the hubs may alter as the type of discount function changes. On the other hand, our results show that (see Fig. 4) the network configuration resulting from using a flow-dependent economies of scale can be much different from that of the case where the classical fixed (flow-independent) discount factor is used.

6. Conclusions

In this paper, a risk-averse single allocation hub location problem with flow-dependent economies of scale was addressed using the mean-CVaR risk measure. It was assumed that the transportation cost on each network arc follows a piece-wise concave function

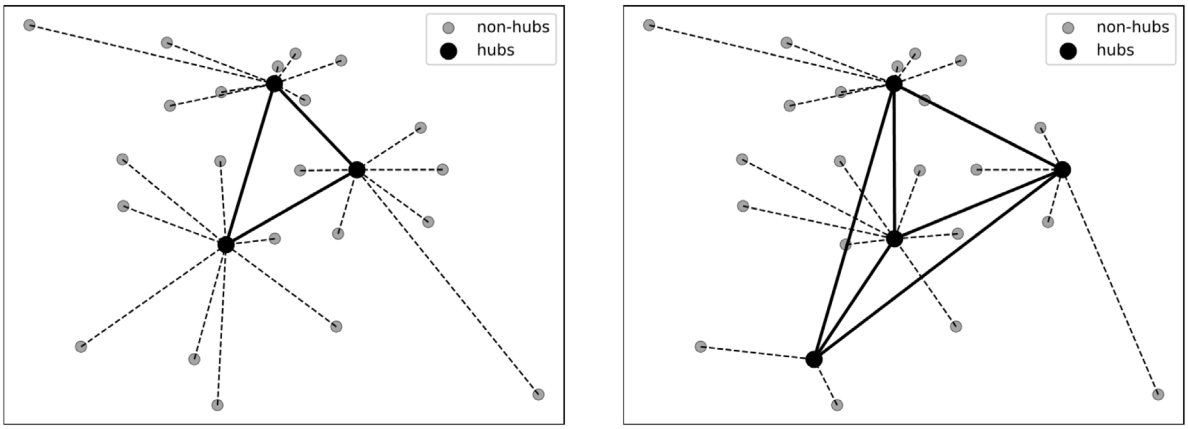

(a) solution with flow-dependent discount (b) solution with fixed discount

Fig. 4. Changes in the network configuration for flow-dependent and fixed discount schemes with the AP25L data set for cost function F3, $\lambda = 0.75$, and $\gamma = 0.8$.

of traffic volume to be transported on that arc. The problem was formulated as a risk-averse two-stage stochastic model and a Benders decomposition algorithm combined with scenario grouping technique was proposed for solving it. The standard implementation of the Benders algorithm was enhanced by applying a number of refinement techniques such as using cut disaggregation schemes, and an efficient two-phase algorithm developed for solving the dual subproblems without calling off-the-shelf optimization packages. Furthermore, a modern implementation of the algorithm was used to solve the problem on a single search tree in which the Benders cuts were successively added on the fly within a branch-and-cut framework. An extensive set of computational experiments was conducted on a well-known data set from the literature with up to 75 nodes. The proposed algorithm was shown to be able to solve all the tested instances in reasonable computational time. Moreover, by altering the values of different input parameters, we studied the resulting changes on the optimal solution of the problem.

As an interesting research direction for future studies, one can consider other sources of uncertainty in the problem data such as transportation costs, fixed setup costs, etc. In addition, the assumption of complete network on the inter-hub level can be relaxed and a more realistic incomplete network can be used for transportation between hubs.

CRediT authorship contribution statement

Nader Ghaffarinasab: Conceptualization, Methodology, Software, Investigation, Writing – original draft. **Özlem Çavuş:** Conceptualization, Supervision, Validation, Reviewing and editing. **Bahar Y. Kara:** Conceptualization, Supervision, Validation, Computing resources, Reviewing and editing.

References

Ahmed, S., 2013. A scenario decomposition algorithm for 0–1 stochastic programs. Oper. Res. Lett. 41 (6), 565–569.
Alkaabneh, F., Diabat, A., Elhedhli, S., 2019. A Lagrangian heuristic and GRASP for the hub-and-spoke network system with economies-of-scale and congestion. Transp. Res. C 102, 249–273.
Alumur, S.A., Campbell, J.F., Contreras, I., Kara, B.Y., Marianov, V., O'Kelly, M.E., 2021. Perspectives on modeling hub location problems. European J. Oper. Res. 291 (1), 1–17.
Alumur, S., Kara, B.Y., 2008. Network hub location problems: The state of the art. European J. Oper. Res. 190 (1), 1–21.
Alumur, S.A., Nickel, S., da Gama, F.S., 2012. Hub location under uncertainty. Transp. Res. B 46 (4), 529–543.
Artzner, P., Delbaen, F., Eber, J.-M., Heath, D., 1999. Coherent measures of risk. Math. Finance 9 (3), 203–228.
Azizi, N., Vidyarthi, N., Chauhan, S.S., 2018. Modelling and analysis of hub-and-spoke networks under stochastic demand and congestion. Ann. Oper. Res. 264 (1), 1–40.
Benders, J.F., 1962. Partitioning procedures for solving mixedvariables programming problems. Numer. Math. 4 (1), 238–252.
Campbell, J.F., 2013. Modeling economies of scale in transportation hub networks. In: 2013 46th Hawaii International Conference on System Sciences. IEEE, pp. 1154–1163.
Campbell, J., Miranda, G.D., Camargo, R.D., O'Kelly, M., 2015. Hub location and network design with fixed and variable costs. In: System Sciences (HICSS), 2015 48th Hawaii International Conference on. pp. 1059–1067.
Campbell, J.F., O'Kelly, M.E., 2012. Twenty-five years of hub location research. Transp. Sci. 46 (2), 153–169.
Çavuş, Ö., 2019. Risk-averse stochastic orienteering problems. Eskişehir Techn. Univ. J. Sci. Technol. A Appl. Sci. Eng. 20 (3), 346–364.
Chaharsooghi, S., Momayezi, F., Ghaffarinasab, N., 2017. An adaptive large neighborhood search heuristic for solving the reliable multiple allocation hub location problem under hub disruptions. Int. J. Ind. Eng. Comput. 8 (2), 191–202.
Contreras, I., Cordeau, J.-F., Laporte, G., 2011a. Benders decomposition for large-scale uncapacitated hub location. Oper. Res. 59 (6), 1477–1490.
Contreras, I., Cordeau, J.-F., Laporte, G., 2011b. Stochastic uncapacitated hub location problem. European J. Oper. Res. 212 (3), 518–528.
Contreras, I., Cordeau, J.-F., Laporte, G., 2012. Exact solution of large-scale hub location problems with multiple capacity levels. Transp. Sci. 46 (4), 439–459.

Contreras, I., O'Kelly, M., 2019. Hub location problems. In: Location Science. Springer, pp. 327–363.
Correia, I., Nickel, S., da Gama, F.S., 2018. A stochastic multi-period capacitated multiple allocation hub location problem: Formulation and inequalities. Omega 74, 122–134.
de Camargo, R.S., de Miranda, Jr., G., Løkketangen, A., 2013. A new formulation and an exact approach for the many-to-many hub location-routing problem. Appl. Math. Model. 37 (12–13), 7465–7480.
de Camargo, R.S., Jr., G.M., Ferreira, R.P.M., Luna, H.P., 2009a. Multiple allocation hub-and-spoke network design under hub congestion. Comput. Oper. Res. 36 (12), 3097–3106.
de Camargo, R.S., Jr., G.M., Luna, H.P., 2008. Benders decomposition for the uncapacitated multiple allocation hub location problem. Comput. Oper. Res. 35 (4), 1047–1064.
de Camargo, R.S., Jr., G.M., Luna, H.P., 2009b. Benders decomposition for hub location problems with economies of scale. Transp. Sci. 43 (1), 86–97.
de Camargo, R.S., de Miranda Jr., G., Ferreira, R.P., 2011. A hybrid outer-approximation/benders decomposition algorithm for the single allocation hub location problem under congestion. Oper. Res. Lett. 39 (5), 329–337.
de Sá, E.M., de Camargo, R.S., de Miranda, Jr., G., 2013. An improved benders decomposition algorithm for the tree of hubs location problem. European J. Oper. Res. 226 (2), 185–202.
de Sá, E.M., Contreras, I., Cordeau, J.-F., de Camargo, R.S., de Miranda Jr., G., 2015. The hub line location problem. Transp. Sci. 49 (3), 500–518.
de Sá, E.M., Morabito, R., de Camargo, R.S., 2018a. Benders decomposition applied to a robust multiple allocation incomplete hub location problem. Comput. Oper. Res. 89, 31–50.
de Sá, E.M., Morabito, R., de Camargo, R.S., 2018b. Efficient Benders decomposition algorithms for the robust multiple allocation incomplete hub location problem with service time requirements. Expert Syst. Appl. 93, 50–61.
Delbaen, F., 2002. Coherent risk measures on general probability spaces. In: Advances in Finance and Stochastics. Springer, pp. 1–37.
Elçi, Ö., Noyan, N., 2018. A chance-constrained two-stage stochastic programming model for humanitarian relief network design. Transp. Res. B 108, 55–83.
Ernst, A.T., Krishnamoorthy, M., 1996. Efficient algorithms for the uncapacitated single allocation p-hub median problem. Locat. Sci. 4 (3), 139–154.
Farahani, R.Z., Hekmatfar, M., Arabani, A.B., Nikbakhsh, E., 2013. Hub location problems: A review of models, classification, solution techniques, and applications. Comput. Ind. Eng. 64 (4), 1096–1109.
Filippi, C., Guastaroba, G., Speranza, M.G., 2020. Conditional value-at-risk beyond finance: a survey. Int. Trans. Oper. Res. 27 (3), 1277–1319.
Gelareh, S., Monemi, R.N., Nickel, S., 2015. Multi-period hub location problems in transportation. Transp. Res. E Logist. Transp. Rev. 75, 67–94.
Gelareh, S., Nickel, S., 2008. A benders decomposition for hub location problems arising in public transport. In: Kalcsics, J., Nickel, S. (Eds.), Operations Research Proceedings 2007: Selected Papers of the Annual International Conference of the German Operations Research Society (GOR) Saarbrücken, September 5–7, 2007. Springer Berlin Heidelberg, Berlin, Heidelberg, pp. 129–134.
Gelareh, S., Nickel, S., 2011. Hub location problems in transportation networks. Transp. Res. 47 (6), 1092–1111.
Ghaffari-Nasab, N., Ghazanfari, M., Teimoury, E., 2015. Robust optimization approach to the design of hub-and-spoke networks. Int. J. Adv. Manuf. Technol. 76 (5–8), 1091–1110.
Ghaffarinasab, N., 2018. An efficient matheuristic for the robust multiple allocation p-hub median problem under polyhedral demand uncertainty. Comput. Oper. Res. 97, 31–47.
Ghaffarinasab, N., 2020. A highly efficient exact algorithm for the uncapacitated multiple allocation p-hub center problem. Decis. Sci. Lett. 9 (2), 181–192.
Ghaffarinasab, N., 2022. Exact algorithms for the robust uncapacitated multiple allocation p-hub median problem. Optim. Lett. 16, 1745–1772.
Ghaffarinasab, N., Andaryan, A.Z., Torkayesh, A.E., 2019. Robust single allocation p-hub median problem under hose and hybrid demand uncertainties: Models and algorithms. Int. J. Manage. Sci. Eng. Manage. 14 (4).
Ghaffarinasab, N., Kara, B.Y., 2019. Benders decomposition algorithms for two variants of the single allocation hub location problem. Netw. Spat. Econ. 19 (1), 83–108.
Ghaffarinasab, N., Kara, B.Y., 2022. A conditional β-mean approach to risk-averse stochastic multiple allocation hub location problems. Transp. Res. E Logist. Transp. Rev. 158, 102602.
Ghaffarinasab, N., Kara, B.Y., Campbell, J.F., 2022. The stratified p-hub center and p-hub maximal covering problems. Transp. Res. B 157, 120–148.
Ghezavati, V., Hosseinifar, P., 2018. Application of efficient metaheuristics to solve a new bi-objective optimization model for hub facility location problem considering value at risk criterion. Soft Comput. 22 (1), 195–212.
Golpîra, H., Zandieh, M., Najafi, E., Sadi-Nezhad, S., 2017. A multi-objective, multi-echelon green supply chain network design problem with risk-averse retailers in an uncertain environment. Sci. Iranica. Trans. E Ind. Eng. 24 (1), 413.
Hosseini, S.D., Verma, M., 2018. Conditional value-at-risk (CVaR) methodology to optimal train configuration and routing of rail hazmat shipments. Transp. Res. B 110, 79–103.
Kargar, K., Mahmutoğulları, A.İ., 2022. Risk-averse hub location: Formulation and solution approach. Comput. Oper. Res. 105760.
Kayışoğlu, B., Akgün, İ., 2021. Multiple allocation tree of hubs location problem for non-complete networks. Comput. Oper. Res. 136, 105478.
Kimms, A., 2006. Economies of scale in hub & spoke network design models: We have it all wrong. In: Morlock, M., Schwindt, C., Trautmann, N., Zimmermann, J. (Eds.), Perspectives on Operations Research. Deutscher Universitats-Verlag, pp. 293–317.
Klincewicz, J.G., 2012. Enumeration and search procedures for a hub location problem with economies of scale. Ann. Oper. Res. 110 (1–4), 107–122.
Lüer-Villagra, A., Eiselt, H., Marianov, V., 2019. A single allocation p-hub median problem with general piecewise-linear costs in arcs. Comput. Ind. Eng. 128, 477–491.
Magnanti, T.L., Wong, R.T., 1981. Accelerating benders decomposition: Algorithmic enhancement and model selection criteria. Oper. Res. 29 (3), 464–484.
Mahmutoğulları, A.İ., Çavuş, Ö., Aktürk, M.S., 2018. Bounds on risk-averse mixed-integer multi-stage stochastic programming problems with mean-CVaR. European J. Oper. Res. 266 (2), 595–608.
Mahmutoğulları, A.İ., Çavuş, Ö., Aktürk, M.S., 2019. An exact solution approach for risk-averse mixed-integer multi-stage stochastic programming problems. Ann. Oper. Res. 1–22.
Marianov, V., Serra, D., 2003. Location models for airline hubs behaving as M/D/c queues. Comput. Oper. Res. 30 (7), 983–1003.
McShan, S., Windle, R., 1989. The implications of hub-and-spoke routing for airline costs. Logist. Transp. Rev. 25 (3), 209.
Meraklı, M., Yaman, H., 2016. Robust intermodal hub location under polyhedral demand uncertainty. Transp. Res. B 86, 66–85.
Meraklı, M., Yaman, H., 2017. A capacitated hub location problem under hose demand uncertainty. Comput. Oper. Res. 88, 58–70.
Najy, W., Diabat, A., 2020. Benders decomposition for multiple-allocation hub-and-spoke network design with economies of scale and node congestion. Transp. Res. B 133, 62–84.
Noyan, N., 2012. Risk-averse two-stage stochastic programming with an application to disaster management. Comput. Oper. Res. 39 (3), 541–559.
O'Kelly, M.E., 1986. The location of interacting hub facilities. Transp. Sci. 20 (2), 92–106.
O'Kelly, M.E., 1987. A quadratic integer program for the location of interacting hub facilities. European J. Oper. Res. 32 (3), 393–404.
O'Kelly, M.E., Bryan, D., 1998. Hub location with flow economies of scale. Transp. Res. B 32 (8), 605–616.
O'Kelly, M.E., Campbell, J.F., de Camargo, R.S., de Miranda, G., 2015. Multiple allocation hub location model with fixed arc costs. Geogr. Anal. 47 (1), 73–96.
Peiró, J., Corberán, Á., Martí, R., Saldanha-da Gama, F., 2019. Heuristic solutions for a class of stochastic uncapacitated p-hub median problems. Transp. Sci. 53 (4), 1126–1149.
Racunica, I., Wynter, L., 2005. Optimal location of intermodal freight hubs. Transp. Res. B 39 (5), 453–477.

Rockafellar, R.T., Uryasev, S., 2000. Optimization of conditional value-at-risk. J. Risk 2, 21–42.
Rockafellar, R.T., Uryasev, S., 2002. Conditional value-at-risk for general loss distributions. J. Bank. Financ. 26 (7), 1443–1471.
Rostami, B., Chitsaz, M., Arslan, O., Laporte, G., Lodi, A., 2022. Single allocation hub location with heterogeneous economies of scale. Oper. Res. 70 (2), 766–785.
Rostami, B., Kämmerling, N., Naoum-Sawaya, J., Buchheim, C., Clausen, U., 2021. Stochastic single-allocation hub location. European J. Oper. Res. 289 (3), 1087–1106.
Sandıkçı, B., Kong, N., Schaefer, A.J., 2013. A hierarchy of bounds for stochastic mixed-integer programs. Math. Program. 138 (1–2), 253–272.
Shahabi, M., Unnikrishnan, A., 2014. Robust hub network design problem. Transp. Res. E Logist. Transp. Rev. 70, 356–373.
Shang, X., Yang, K., Jia, B., Gao, Z., 2021. The stochastic multi-modal hub location problem with direct link strategy and multiple capacity levels for cargo delivery systems. Transportmetrica A Transp. Sci. 17 (4), 380–410.
Sim, T., Lowe, T.J., Thomas, B.W., 2009. The stochastic p-hub center problem with service-level constraints. Comput. Oper. Res. 36 (12), 3166–3177.
Taherkhani, G., Alumur, S.A., Hosseini, M., 2020. Benders decomposition for the profit maximizing capacitated hub location problem with multiple demand classes. Transp. Sci. 54 (6), 1446–1470.
Taherkhani, G., Alumur, S.A., Hosseini, M., 2021. Robust stochastic models for profit-maximizing hub location problems. Transp. Sci. 55 (6), 1322–1350.
Tanash, M., Contreras, I., Vidyarthi, N., 2017. An exact algorithm for the modular hub location problem with single assignments. Comput. Oper. Res. 85, 32–44.
Yang, T.-H., 2009. Stochastic air freight hub location and flight routes planning. Appl. Math. Model. 33 (12), 4424–4430.
Yang, K., Liu, Y., Yang, G., 2014. Optimizing fuzzy p-hub center problem with generalized value-at-risk criterion. Appl. Math. Model. 38 (15–16), 3987–4005.
Yang, K., Yang, L., Gao, Z., 2017. Hub-and-spoke network design problem under uncertainty considering financial and service issues: A two-phase approach. Inform. Sci. 402, 15–34.
Yu, G., Haskell, W.B., Liu, Y., 2017. Resilient facility location against the risk of disruptions. Transp. Res. B 104, 82–105.
Zetina, C.A., Contreras, I., Cordeau, J.-F., Nikbakhsh, E., 2017. Robust uncapacitated hub location. Transp. Res. B 106, 393–410.
Zhai, H., Liu, Y., Chen, W., 2012. Applying minimum-risk criterion to stochastic hub location problems. Procedia Eng. 29, 2313–2321, 2012 International Workshop on Information and Electronics Engineering.